Bidirectional crosstalk between HIF and Glucocorticoid signalling in zebrafish larvae

Davide Marchi[1*], Kirankumar Santhakumar[5], Eleanor Markham[1], Nan Li[2], Karl-Heinz Storbeck[3], Nils Krone[2,4], Vincent T. Cunliffe[1] and Fredericus J.M. van Eeden[1**]

[1]The Bateson Centre & Department of Biomedical Science, Firth Court, University of Sheffield, Western Bank, Sheffield, S10 2TN, United Kingdom. [2]The Bateson Centre & Department of Oncology and Metabolism, School of Medicine, University of Sheffield, Sheffield, S10 2TH, United Kingdom. [3]Department of Biochemistry, Stellenbosch University, Stellenbosch, 7602, Matieland, South Africa. [4]Department of Medicine III, University Hospital Carl Gustav Carus, Technische Universität Dresden, Fetscherstrasse 74, 01307 Dresden, Germany. [5]Department of Genetic Engineering, SRM Institute of Science and Technology Kattankulathur 603 203, India.

*Corresponding author. Tel: +44 1142 24653; E-mail: dmarchi1@sheffield.ac.uk
**Corresponding author. Tel: +44 1142 222348; E-mail: f.j.vaneeden@sheffield.ac.uk

Abstract

In the last decades few *in vitro* studies highlighted the potential for cross-talk between hypoxia inducible factor-(HIF) and glucocorticoid-(GC) signalling pathways. However, how this interplay precisely occurs *in vivo* is still debated. Here, we use zebrafish larvae (*Danio rerio*) to elucidate how and to what degree hypoxic signalling affects the endogenous glucocorticoid pathway and *vice versa, in vivo*. Firstly, our results demonstrate that in the presence of upregulated HIF signalling, both glucocorticoid response and endogenous cortisol levels are repressed in 5 days post fertilisation larvae. In addition, despite HIF activity being low at normoxia, our data show that it already impedes glucocorticoid activity and levels. Secondly, we further analysed the *in vivo* contribution of glucocorticoids to HIF signalling. Interestingly, our results show that both glucocorticoid receptor (GR) and mineralocorticoid receptor (MR) play a key role in enhancing the HIF response. Finally, we found indications that glucocorticoids promote HIF signalling via multiple routes. Cumulatively, our findings allowed us to suggest a model for how this cross-talk occurs *in vivo*.

Keywords: glucocorticoid signaling, hypoxia inducible factor, vhl, zebrafish, hypotalamus-pituitary-interrenal axis, metabolism, negative feedback, liver.

Subject Categories Developmental biology; Endocrinology; Metabolism.

Introduction

Glucocorticoids constitute a well-characterized class of lipophilic steroid hormones produced by the adrenal glands in humans and by the interrenal tissue in teleosts. The circadian production of glucocorticoids in teleosts is regulated by the hypothalamus-pituitary-interrenal (HPI) axis, which is the equivalent of the mammalian hypothalamus-pituitary-adrenal (HPA) axis. Both are central to stress adaptation (Alsop and Vijayan, 2009; Griffiths *et al.*, 2012; Tokarz *et al.*, 2013; Faught and Vijayan, 2018). Glucocorticoids exert their function via direct binding to the intracellular glucocorticoid receptor (GR) (Bamberger, Schulte and Chrousos, 1996), and together act as a transcription factor, which can function either in a genomic or in non-genomic way (Stahn and Buttgereit, 2008; Mitre-Aguilar, *et al.*, 2015; Facchinello *et al.*, 2017; Panettieri *et al.*, 2019)

Hypoxia-inducible factor (HIF) transcription factors are key regulators of the cellular response to hypoxia, which coordinate a metabolic shift from aerobic to anaerobic metabolism in the presence of low oxygen availability in order to assure homeostasis (Semenza, 2011). Hypoxia, is a common pathophysiological condition (Bertout, Patel and Simon, 2008; Semenza, 2013) to which cells must promptly respond in order to avert metabolic shutdown and subsequent death (Elks *et al.*, 2015). In the presence of normal oxygen levels, a set of prolyl hydroxylases (PHD1, 2 and 3) use the available molecular oxygen directly to hydroxylate HIF-α subunit. Hydroxylated HIF-α is then recognised by the Von Hippel Lindau (VHL) protein, which acts as the substrate recognition part of a E3-ubiquitin ligase complex. This leads to HIF-α proteasomal degradation to avoid HIF pathway activation under normoxic conditions. On the other hand, low O_2 levels impair the activity of the PHDs enzymes leading to HIF-α stabilisation and subsequent translocation in the nucleus. Here, together with HIF-β subunit, HIF-α forms a functional transcription complex, which drives the hypoxic response (Semenza, 2012). Although the HIF response is aimed to restore tissue oxygenation and perfusion, it can sometimes be maladaptive and can contribute to a variety of pathological conditions including inflammation, tissue ischemia, stroke and growth of solid tumours (Cummins and Taylor, 2005). Finally, it is important to note for this study that HIF signalling is able to regulate its own activation via negative feedback, by inducing the expression of PHD genes, in particular prolyl hydroxylase 3 (PHD3) (Pescador *et al.*, 2005; Santhakumar *et al.*, 2012).

The presence of a cross-talk between glucocorticoids and hypoxia dependent signalling (HIF) pathways has been widely demonstrated by several *in vitro* studies (Kodama *et al.*, 2003; Leonard *et al.*, 2005; Wagner *et al.*, 2008; Zhang *et al.*, 2015, 2016). Moreover, synthetic glucocorticoids (ie. betamethasone and dexamethasone), which are analogous to naturally occurring steroid hormones, have been extensively used for decades as anti-inflammatory drugs for treating pathological conditions which are linked to hypoxia (i.e. asthma, rheumatoid arthritis, ischemic injury, etc.) (Nikolaus, Fölscn and Schreiber, 2000; Neeck, Renkawitz and Eggert, 2002; Busillo and Cidlowski, 2013). However, due to the presence of adverse effects (Moghadam-Kia and Werth, 2010) and glucocorticoid resistance (Barnes and Adcock, 2009; Barnes, 2011), their use has been limited. Therefore, extending the research on how precisely this interplay occurs *in vivo*, may have a wide physiological significance in health and disease.

The first evidence of interaction between HIF and GR was provided by Kodama et al. 2003, who discovered that ligand-dependent activation of glucocorticoid receptor enhances hypoxia-dependent gene expression and hypoxia response element (HRE) activity in HeLa cells. Leonard et al. 2005 subsequently revealed that GR is transcriptionally upregulated by hypoxia in human renal proximal tubular epithelial cells. Furthermore, the hypoxic upregulation of GR was confirmed by Zhang et al 2015. In contrast, a dexamethasone-mediated inhibition of HIF-1α target genes expression in hypoxic HEPG2 cells was demonstrated by Wagner et al. 2008. In addition to that, they showed retention of HIF-1α in the cytoplasm, suggesting a blockage in nuclear import. Finally, Gaber *et al.*, 2011 indicated the presence of dexamethasone-induced suppression of HIF-1α protein expression, which resulted in reduced HIF-1 target gene expression.

From these *in vitro* results it has become clear that HIF-GCs cross-talk is complex and may depend on cell type. In the present study, we have used the zebrafish (*Danio rerio*) as an *in vivo* model organism to study how and to what degree hypoxic signalling affects the endogenous glucocorticoids' response and vice versa. The use of whole animals allows us to show how these signals interact at a more global level than in cell culture, where interactions between different tissues and cell types are not easily modelled. The zebrafish offers an excellent genetic vertebrate model system for endocrine studies, and similar to humans, they are diurnal and use cortisol as the main glucocorticoid hormone (Weger *et al.*, 2016). Importantly, unlike other teleosts, zebrafish have only a single glucocorticoid (zGr) and mineralocorticoid receptor (Mr) (zMr) isoform (Faught and Vijayan, 2018). Moreover, zGr shares high structural and functional

similarities to its human equivalent, making zebrafish a reliable model for studying glucocorticoids activity *in vivo* (Alsop and Vijayan, 2008; Chatzopoulou *et al.*, 2015; Xie *et al.*, 2019). Additionally, zebrafish share all the components of the human HIF signalling pathway and it has been proved to be a very informative and genetically tractable organism for studying hypoxia and HIF pathway both in physiological and pathophysiological conditions (van Rooijen *et al.*, 2011; Santhakumar *et al.*, 2012; Elks *et al.*, 2015).

In our previous work, we identified new activators of the HIF pathway, e.g. betamethasone, a synthetic glucocorticoid drug (Vettori *et al.*, 2017). Counterintuitively, GR loss of function was shown by Facchinello and colleagues to hamper the transcriptional activity linked to immune-response (i.e of cytokines Il1β, Il8 and Il6 and of the metalloproteinase Mmp-13) (Facchinello *et al.*, 2017). Finally, glucocorticoid receptor has been also found to synergistically activate proinflammatory genes by interacting with other signalling pathways (Langlais *et al.*, 2008, 2012; Dittrich *et al.*, 2012; Xie *et al.*, 2019).

In the present study, we utilised both a genetic and pharmacological approach to alter these two pathways during the first 120 hours post fertilisation of zebrafish embryos. In particular, we took advantage of two different mutant lines we have generated (*hif1β*^{sh544} (*Arnt1*) and *gr*^{sh543} (*nr3c1*) respectively), coupled to an already existing *vhl*$^{hu2117/+}$*;phd3::EGFP*$^{i144/i144}$ hypoxia reporter line (Santhakumar *et al.*, 2012), to study the effect of HIF response on GCs signalling and vice-versa, via a "gain-of-function/loss-of-function" approach. Phenotypic and molecular analyses of these mutants have been accompanied by optical and fluorescence microscope imaging.

Importantly, we not only confirm that betamethasone is able to increase the expression of *phd3:eGFP*, a marker of HIF activation in our zebrafish HIF-reporter line, but we also show that BME-driven HIF response requires Hif1β/Arnt1 action to occur. Furthermore, our results also demonstrate that both Gr and Mr loss of function are able to partially rescue *vhl* phenotype, allowing us to confirm the importance of glucocorticoids in assuring a proper HIF response.

Our results also demonstrate that in the presence of upregulated HIF pathway (by mutating *vhl*), both glucocorticoid response and the endogenous cortisol levels are repressed in 5 dpf larvae, whereas when HIF pathway is suppressed (by mutating *hif1β*) they are significantly increased. Finally, qPCR analysis on GCs target genes, *in situ*

hybridisation on the expression of steroidogenic genes and cortisol quantification on the aforementioned mutant lines confirmed our hypothesis.

Taken together, these results allow us to deepen the knowledge of how the cross-talk between HIF and glucocorticoid pathway occurs *in vivo* and to underscore a new model of interaction between these two major signalling pathways.

Materials and methods

Zebrafish husbandry and maintenance:

Zebrafish (Danio rerio) lines were raised and maintained under standard conditions (14 hours of light and 10 hours of dark cycle, at 28°C) in the Aquaria facility of the University of Sheffield. Zebrafish embryos used for experiments were reared in E3 medium (5 mM NaCl, 0,17 mM KCl, 0,33 mM MgCl2, 0,33 mM CaCl2, pH 7,2) with or without methylene blue (Sigma-Aldrich) and staged according to standard methods (Kimmel *et al.*, 1995) for up to 5,2 days post fertilisation (dpf) in accordance with UK Home Office legislation. Experiments performed on zebrafish embryos conformed to UK Home Office regulations.

Zebrafish strains:

The following zebrafish lines were used: wild-type (wt) strain AB (ZDB-GENO-960809-7), *vhl*$^{hu2117/+}$;*phd3*:eGFP$^{i144/i144}$ (ZDB-GENO-090611-18), *hif1β*$^{sh544/+}$; *hif1β*$^{sh544/+}$;*vhl*$^{hu2117/+}$, *gr*$^{sh543/+}$, *gr*$^{sh543/+}$;*vhl*$^{hu2117/+}$, *gr*$^{sh543/+}$;*hif1β*$^{sh544/+}$; and *gr*$^{sh543/+}$;*hif1β*$^{sh544/+}$;*vhl*$^{hu2117/+}$ lines were generally maintained in a *phd3:EGFP*$^{i144/+}$ background. The following 4x gRNAs CRISPR-injected G0 null mutant lines were created according to Wu et al, 2018 protocol and raised up to to 5,2 dpf: *mr;gr*$^{sh543/+}$;*vhl*$^{hu2117/+}$;*phd3:eGFP*$^{i144/+}$, *hif1β2;1hif1β*$^{sh544/+}$;*vhl*$^{hu2117/+}$;*phd3:eGFP*$^{i144/+}$ and *lamb1b;vhl*$^{hu2117/+}$;*phd3:eGFP*$^{i144/+}$ (used as CRISPR injection control).

Generation of *gr* (*nr3c1*) and *hif1β* (*arnt1*) null zebrafish lines:

Both *nr3c1* mutant line (*gr*$^{sh543/+}$) and *arnt1* mutant line (*hif1β*$^{sh544/+}$) were generated using the CRISPR/Cas9-based mutagenesis method. A gene-specific guide RNA (sgRNA) sequence was identified using the CHOPCHOP website (Montague *et al.*, 2014; Labun *et al.*, 2016). To design both *gr* and *arnt1* sgRNA, an 18 nucleotides sequence upstream to a selected PAM site (*gr*$^{sh543:}$ CCAGCTGACGATGTGGCAG; *hif1β*^{sh544}: TCGGTGCTGGTGTTTCCAG) was inserted into a scaffold sequence (Hruscha *et al.*, 2013),

containing a promoter for the T7 Polymerase. The sgRNA was amplified via PCR, purified from agarose gel and *in vitro* transcribed using MEGAshortscript T7 kit (Ambion). 1 nl of CRISPR mixture containing 2,4 µg/µl of gRNA and 0,5 µl Cas9 protein (NEB) was injected in one-cell stage embryos and raised for 24 hours. Wild-type (wt), strain AB embryos were used to generate the *gr* mutant line, whereas *vhl*$^{hu2117/+}$*;phd3:eGFP*$^{i144/+}$ incross-derived embryos were used to create the *hif1β* mutant line. Efficiency was verified via whole-embryo PCR-based genotyping, by a diagnostic restriction digest. Injected embryos were raised to adulthood. Embryos collected from transmitting G0 founders crossed with WT(AB) fish were raised and genotyped to confirm germline transmission of the mutation (F1 generation). Heterozygous mutants, carrying the same mutation, were selected and crossed to obtain homozygous mutant embryos (F2 generation).

Generation of CRISPR/Cas9-mediated mutants (CRISPANTs):

To generate G0 knockout embryos we used the method developed by Wu et al., 2018. In short, a pool of four guide-RNAs (25µM each, Sigma Aldrich) were co-injected with 0,5 µl Cas9 protein (NEB, M0386, 20µM), diluted 1:10) and 1 µl tracrRNA (100µM) in one-cell stage embryos. This method was used to create G0 CRISPANTs for the following genes of interest: *mineralocorticoid receptor* (*mr, nr3c2*), *aryl hydrocarbon receptor nuclear translocator 2* (*arnt2, hif1β2*) and *laminin, beta 1b* (*lamb1b*). The latter was used as CRISPR-injection control. The gRNA target sequences used in this study are as follows: *arnt2*: gRNA1- ACGGCGCCTACAAACCCTCC, gRNA2- GGCCGATGGCTTCTTGTTCG, gRNA3- TTCACGCCACAATTCGGATG, gRNA4- GTCGCAGGTGCGTAAAAACA; *nr3c2:* gRNA1- GCATTGTGGGGTCACCTCCA, gRNA2- AAGGGGATTAAACAGGAAAC, gRNA3- CAACCAGCTCGCCGGAAAAC, gRNA4- ATATCTGACGCCGTCCGTCT; *lamb1b* gRNA1- TTGTTAATAGCATAGTACATTGG, gRNA2- GGAGAACAAGCAAAACGATGAGG, gRNA3- GCGTGGTGCAGGGTTTGTAG, gRNA4- TCACAATGACATGTGTGCG. The success of the injection was determined via phenotypic analysis, followed by quantification of *phd3:eGFP* related brightness and whole-embryo PCR-based genotyping performed on a fraction of injected embryos at 5 dpf .

Whole-mount *in situ* hybridisation:

Whole-mount *in situ* hybridization (WISH) was performed according to standard protocols (Thisse and Thisse, 2008). The following antisense RNA probes were used: *proopiomelanocortin a* (*pomca*) created as previously described (Muthu *et al.*, 2016);

Cytochrome P450 family 17 polypeptide 2 (cyp17a2), created as previously described (Eachus *et al.*, 2017), both *prolyl hydroxylase 3 (phd3; BC066699),* and *lactate dehydrogenase A (ldha1; BC067188)* probes*,* generated as previously described (van Rooijen *et al.*, 2009; Santhakumar *et al.*, 2012).

Embryos harvesting, drug treatment and fixation for WISH:

Embryos intended for whole-mount *in situ* hybridisation were treated with 16,8 µl of 1-phenyl 2-thiourea (PTU, stock concentration 75mg/ml) diluted into 35 ml E3 medium to inhibit melanogenesis, according to Karlsson et al., 2001. GR agonist treatment was performed on batches of 15 embryos each, at 4 dpf, treated in 6-well plates, with 30 µM Betamethasone 17,21-dipropanoate (BME) and with 1% DMSO (Sigma-Aldrich), as control, for 24 hours (Griffiths et al., 2012). Inside the 6-well plates, embryos were incubated in 3 ml total volume of E3 medium, without methylene blue. Afterwards, up to 30 embryos at 5 dpf were collected in 1,5 ml Eppendorf tubes and anaesthetized using Tricaine Solution (MS-222, Sigma Aldrich) prior to fixation in 1 ml 4% PFA solution overnight, at 4°C. Embryos were then washed twice for 10 minutes in PBST and post-fixed in 1 ml 100% MeOH. Finally, samples were stored at -20°C.

***gr*^{sh543} mutants sorting by visual background adaptation (VBA):**

Visual background adaptation (VBA) is a glucocorticoid receptor-dependent neuroendocrine response which causes zebrafish melanocytes to shrink when exposed to bright illumination (Kramer *et al.*, 2001; Kurrasch *et al.*, 2009). To identify *gr*^{sh543} mutants from siblings and to confirm the absence of a functional VBA response, 5dpf larvae were exposed to 30 minutes darkness and then transferred onto a white background under bright, whole-field illumination, using a 30W fluorescent lamp mounted 50 cm above the dish (Muto *et al.*, 2005; Hatamoto and Shingyoji, 2008).

Cortisol extraction and quantification:

Cortisol quantification was carried out according to the protocol published by Eachus *et al.*, 2017 . Three biological replicates of 150 larvae at 5dpf each of *hif1β*^{sh544} mutants, *hif1β*^{sh544} siblings, *vhl*^{hu2117} mutants and *vhl*^{hu2117} siblings, respectively, were used for steroid hormone extraction and quantification.

RNA isolation, cDNA synthesis and qPCR analysis:

Transcript abundance of target genes was measured by quantitative real-time PCR (RTqPCR). Three biological replicates of 10 larvae at 4 dpf each, were treated for 24 hours with 30 μM Betamethasone 17,21-dipropanoate and with 1% DMSO, used as control, prior to RNA isolation. Total RNA was extracted from pools of 10 larvae at 5dpf with TRIzol reagent (Invitrogen by Thermo Fisher Scientific, 15596026). RNA extracted was quantified using a Nanodrop ND-1000 spectrophotometer. cDNA was then synthesized from 1μg RNA template through reverse transcription using Protoscript II First Strand cDNA Synthesis Kit (New England Biolabs), as recommended by manufacturer's instructions. All RTqPCR reactions were performed in triplicate using TaqMan probes™ in combination with CFX96 Touch™ Real-Time PCR Detection System (BioRad), paired with CFX Maestro™ Analysis Software. Each reaction mixture (20 μl) reaction mixture containing 1 μl cDNA template (100ng/ml), 1 μl FAM™ probe and 10 μl TaqMan Universal Master Mix (Applied biosystems by Thermo Fisher Scientific, Epsom, UK) was amplified as follows: denaturation at 95°C for 10 minutes and 39 cycles at 95°C for15 seconds, 60°C for 30 seconds. Four hypoxia-inducible factor pathway-dependent genes (*egln3:* Dr03095294_m1*, pfkfb3: Dr03133482_m1, vegfab:* Dr03072613_m1 *and slc2a1a: Dr03103605_m1*) and four glucocorticoid pathway-dependent target genes (*fkbp5: Dr03114487_m1*, *il6st:* Dr03431389_m1*, pck1: Dr03152525_m1 and lipca:* Dr03113728_m1) were quantified in the present study (Applied biosystems by Thermo Fisher Scientific, Epsom, UK). Expression levels for each gene were normalized to e*ef1a1* (Dr03432748_m1) and/or *rps29* (Dr03152131_m1) and fold change values were generated relative to wild-type DMSO treated control levels, according to ΔΔCT method (Livak and Schmittgen, 2001). All data were expressed as fold change mean ± s.e.m and $P \leqslant 0.05$ was considered statistically significant.

Quantifying *phd3:eGFP*-related brightness:

Images were acquired using Leica Application Suite version 4.9, which allowed the capture of both bright-field and GFP fluorescent images. To quantify the *phd3:eGFP*-related brightness of live embryos derived from each incrossed mutant line used in this project, Fiji (Image J) software v.2.0.0 was used. Images were converted into a grey scale 8-bit format and subsequently analysed by the software, by summing the grey values of all the pixels in the selected area, divided by the number of pixels. By default, since values equal 0 are assigned to black and values equal to 255 to white, the quantified mean grey

values are proportional to the intensity of the eGFP-related brightness expressed in the embryos. In particular, head, liver and tail (from the anus to the caudal peduncle) related brightness were selected and measured in all the mutant lines used in this study.

Statistical analysis:

GraphPad Prism version 8.0 for MacOS (GraphPad Software, La Jolla, California, USA, www.graphpad.com) was used to perform statistical analysis on all the samples analysed. Unpaired t tests were used to test for significant differences between two sample groups (i.e cortisol quantification). One-way ANOVA was used for assessing mean grey values data quantification, whereas two-way ANOVA was used to evaluate qPCR data. As post-hoc correction tests, Sidak's method for multiple comparisons was used on normally distributed populations following one-way ANOVA, while Dunnett's correction was used for comparing every mean to a control mean, on normally distributed populations following two-way ANOVA.

Results

Generating *arnt1* and *arnt1;vhl* knockout in zebrafish:

To study the interplay between HIF and GC signalling *in vivo,* using a genetic approach, we required an Hif1β/Arnt1 mutant line (in a *phd3:eGFP*;$vhl^{+/-}$ background) to enable the downregulation HIF signalling. Hif-1β (hypoxia-inducible factor 1 beta, Arnt1) is a nuclear receptor that is targeted by and bound to Hif-α subunits, when the latter migrate into the nucleus after its stabilization in the cytoplasm. It represents the most downstream protein in the HIF pathway and for this reason it is the most suitable target. Using CRISPR mutagenesis we obtained a 7 bp insertion in exon 5 (coding bHLH DNA binding domain (DBD) of the Hif-1β protein; allele name sh544) in *vhl* heterozygote embryos (**Fig.1a**). The resulting frameshift mutation was predicted to lead to a premature stop codon at the level of the DNA-binding domain, which would result in a severely truncated protein. The resulting line $hif1\beta^{sh544/+};vhl^{hu2117/+};phd3:eGFP^{i144/i144}$ will be called $artn1^{+/-};vhl^{+/-}$, whereas the $vhl^{hu2117/+};phd3:eGFP^{i144/i144}$ line will be called $vhl^{+/-}$ hereafter.

Initial analysis performed on $arnt1^{+/-};vhl^{+/-}$ incross-derived 5 dpf larvae (F1 generation) confirmed the suppressive effect that *arnt1* mutation was expected to have on *vhl* mutants. Overall, $arnt1^{-/-};vhl^{-/-}$ larvae showed a substantially attenuated *vhl*

phenotype, characterized by a reduced *phd3:eGFP* related brightness, especially in the liver, with the absence of pericardial edema, excessive caudal vasculature and normal yolk usage compared to *vhl*$^{-/-}$ larvae **(Fig.1b)**. In particular, this was quantified as a 39% downregulation (P<0.0017) at the level of the head, a 75% downregulation (P<0.0001) in liver and a 58% downregulation (P<0.0001) in the rest of the body (from the anus to the caudal peduncle), in terms of *phd3:eGFP*-related brightness, compared to *vhl*$^{-/-}$ larvae (**Fig.1c and Fig.EV1a**).

Furthermore, since homozygous *vhl* mutants are lethal by 8-10dpf (van Rooijen *et al.*, 2009), to analyze the efficacy of *arnt1* mutation in rescuing *vhl* phenotype, we attempted to raise *arnt1*$^{-/-}$;*vhl*$^{-/-}$ after day 5 post fertilization. Notably, double mutants were able to survive beyond 15 dpf, but failed to grow and thrive when compared to their wild-type siblings, which led us to euthanise them due to health concerns at 26 dpf (**Fig.EV1b)**. Of note, *arnt1* homozygotes, in a *vhl*$^{/+}$ or wt background, were morphologically indistinct and adults were viable and fertile. In contrast, the previously published *arnt2*$^{-/-}$ zebrafish larvae were embryonic lethal around 216 hpf (Hill *et al.*, 2009).

Arnt1 and Arnt2 are mutually involved in assuring HIF response in zebrafish:

As arnt1;*vhl* double mutants still activate the *phd3:eGFP* HIF reporter, we examined the importance of Arnt2 isoform in the HIF response. Phenotypic analysis was carried out on 5 dpf Arnt2 CRISPANTs, created both in a *vhl*$^{+/-}$ and *arnt1*$^{+/-}$;*vhl*$^{+/-}$ background, according to the protocol of Wu et al., 2018. By analysing the expression of the *phd3:eGFP* transgene, we observed that *arnt2* CRISPR injected *vhl* mutants were characterized by a significant downregulation of *phd3:eGFP*-related brightness at the level of the head (equals to 53%, P<0.0001), in the liver (equals to 54%, P<0.0001) and in the rest of the body (equals to 46%, P<0.0001), compared to uninjected *vhl* mutant larvae (**Fig.1d,e)**.

Furthermore, when both *arnt1* and *arnt2* isoforms were simultaneously knocked-out, the downregulation was even stronger at the level of the head (equals to 74%, P<0.0001), liver (equals to 86%, P<0.0001) and in the rest of the body (equals to 83%, P<0.0001) (**Fig. 1d,e**). Overall, these data allow to confirm that Arnt1, even if not fundamental for survival, is the main isoform required for HIF signaling at the hepatic level in zebrafish larvae, whereas Arnt2 is more expressed in the developing central nervous system (CNS), as reported by Hill et., al 2009. Of note, since both isoforms can

form a functional complex with HIF-α and appear to function in the same organs, this allows us to confirm that they have partially overlapping functions *in vivo* and to show that they synergistically contribute to the HIF response.

Modulation of HIF signalling affects GR signalling:

To investigate the interaction between HIF and glucocorticoid response, RTqPCR analysis was performed on 5 dpf larvae to quantify the expression of four glucocorticoid target genes (*fkbp5, il6st, pck1 and lipca*) both in a HIF upregulated (*vhl*$^{-/-}$), attenuated (*arnt1*$^{-/-}$;*vhl*$^{-/-}$) and downregulated scenario (*arnt1*$^{-/-}$). Collectively, this analysis showed that the expression of *fkbp5* and *pck1* (two of the main glucocorticoids target genes) is downregulated (fold change=0,1; P=0.0035 and fold change=0,16; P=0.041, respectively) in the presence of a strongly activated HIF pathway (*vhl*$^{-/-}$), whereas only *fkbp5* expression is significantly downregulated (fold change=0,3; P=0.0164) in a HIF attenuated scenario (*arnt1*$^{-/-}$;*vhl*$^{-/-}$), compared to wild-type larvae. In contrast, when HIF levels are suppressed (*arnt1*$^{-/-}$), basal GC signalling (mainly *fkbp5* expression) is upregulated (fold change=8,2; P=0.0004), compared to wild-type levels (**Fig.2a and Fig. EV2**).

To further examine the ability of HIF in repressing GCs response, we performed betamethasone (BME) treatment [30 μM] on the aforementioned mutant lines, followed by RTqPCR analysis. Interestingly, both in the presence of upregulated and partially attenuated HIF levels (*vhl*$^{-/-}$ and *arnt1*$^{-/-}$;*vhl*$^{-/-}$, respectively), BME was not able to significantly increase the expression of all the four glucocorticoid target genes analysed (**Fig. 2a and Fig. EV2**). In contrast, when the HIF pathway was suppressed (*arnt1*$^{-/-}$), BME was able to further upregulate mainly the expression of *fkbp5* (fold change=14,5; P<0,0001), *pck1* (fold change=11,1; P=0,0040) and *il6st* (fold change=5,73; P=0,0041) (**Fig. 2a and Fig. EV2**). Collectively, these results indicate that upregulated HIF is somehow able to repress glucocorticoid response and can strongly blunt or abolish the response to an exogenous GR agonist. Interestingly, although HIF activity is expected to be low in wild-type larvae in a normoxic environment, its function is detectable with respect to suppression of GR activity.

HIF signalling acts as negative regulator of steroidogenesis:

To investigate the relationship between HIF signaling and steroidogenesis, we initially performed *in situ* hybridization on embryos from our *arnt1*$^{+/-}$ mutant line, using

both *pro-opiomelanocortin* (*pomca*) and *Cytochrome P450 family 17 polypeptide 2* (*cyp17a2*) as probes. Expression of *pomca*, at the level of the anterior part of the pituitary gland, is a well-established readout of Gr function in zebrafish larvae. Indeed, it is negatively regulated by increased blood cortisol levels via GC-GR signalling, as part of the HPI axis feedback loop (Griffiths *et al.*, 2012; Ziv *et al.*, 2014). Previous work also suggested that HIF promotes POMC activity in the mouse hypothalamic region (Zhang *et al.*, 2011). On the other hand, Cyp17a2 is an enzyme involved in steroid hormone biosynthesis at the level of interrenal gland, which is activated upon ACTH stimulation (Ramamoorthy and Cidlowski, 2016; Eachus *et al.*, 2017; Weger *et al.*, 2018).

We found that 5 dpf *arnt1*$^{-/-}$ larvae, which were characterized by an upregulated glucocorticoid response, showed upregulated *cyp17a2* expression coupled to downregulated *pomca*. As expected, *arnt1* siblings showed normally expressed *pomca* and *cyp17a2*, which were observed to be downregulated only as a consequence of BME treatment (**Fig. 2b and 2d**). Therefore, we speculate that in the absence of *arnt1*, *pomca* downregulation is most likely to occur as a consequence of GC-GR induced negative feedback loop, triggered by an upregulated glucocorticoid response (**Fig. 2b'**).

We subsequently examined both *pomca* and *cyp17a2* expression in the opposite -HIF upregulated- scenario, by performing *in situ* hybridization on the *vhl* mutant line. Interestingly, 5 dpf *vhl*$^{-/-}$ larvae, which were characterized by a downregulated glucocorticoid response, displayed downregulated *cyp17a2* expression, coupled to downregulated *pomca* expression. On the other hand, *vhl* siblings showed normally expressed *pomca*, which was observed to be downregulated after BME treatment, as expected (**Fig. 2c and 2e**).

As both *fkbp5* and *pck1* (GCs target genes) are downregulated in *vhl* mutants (**Fig. EV2a**), we speculate that by upregulating HIF (*vhl* knock-out larvae), glucocorticoid response is effectively repressed as a consequence of HIF-mediated downregulation of *pomca* expression (**Fig. 2c'**). Cumulatively, if this is true, we predict to observe reduced levels of endogenous cortisol in *vhl*$^{-/-}$and normal or even increased levels in *arnt1*$^{-/-}$ at 5 dpf.

Impaired steroidogenesis in *vhl* mutant zebrafish:

To confirm this hypothesis, we performed cortisol quantification on the aforementioned *vhl* and *arnt1* mutant lines. Indeed, cortisol concentration was significantly reduced (P value <0.0028) in *vhl* mutant larvae (13.9 pg/150 larvae),

compared to *vhl* siblings (48.2 pg/150 larvae). Conversely, cortisol was significantly increased (P value <0.0001) in *arnt1* mutants (66.8 pg/150 larvae), compared to *arnt1* siblings (48.7 pg/150 larvae) (**Fig. 2f**). Taken together, these data show the presence of a strong HIF-induced negative regulation of steroidogenesis and GR activity.

Generating *gr* and *gr;vhl* knockout in zebrafish:

To further investigate the reverse role of glucocorticoids on HIF response, we created a novel glucocorticoid receptor (*gr*, *nr3c1*) mutant line and we crossed it with the *vhl*$^{hu2117/2117}$*;phd3::EGFP*$^{i144/i144}$ hypoxia reporter line (this line will be called *gr*$^{+/-}$*;vhl*$^{+/-}$ hereafter). We created this line because the existing *gr*^{s357} allele may still have some activity via non-genomic pathways or tethering, promoting HIF activation upon GC treatment (Griffiths *et al.*, 2012; Ziv *et al.*, 2012; Vettori *et al.*, 2017). Of note, *gr* mutants are hypercortisolemic (Facchinello *et al.*, 2017; Faught and Vijayan, 2018). This is due to the inability of glucocorticoids to bind to a functional receptor (GR). As a result, they fail to provide negative feedback and are not able to shut down GC biosynthesis (Facchinello *et al.*, 2017; Faught and Vijayan, 2018). We generated an 11 bp deletion at the level of *gr* exon 3, which is predicted to truncate the DNA binding domain, lacks the C-terminal ligand binding domain and is predicted to be a true null (**Fig. 3a)**. The homozygous *gr/nr3c1* mutants, characterized during the first 5dpf, were morphologically similar to control siblings and adult fish were viable and fertile, as predicted (Facchinello *et al.*, 2017).

To confirm loss-of-function, we initially subjected larvae to a visual background adaptation (VBA) test, as VBA is linked to impaired glucocorticoid biosynthesis and action (Griffiths *et al.*, 2012; Muto *et al.*, 2013). Larvae derived from *gr*$^{+/-}$ incross were VBA analyzed and sorted according to melanophore size at 5 dpf. PCR-based genotyping on negative VBA-response sorted samples revealed that most larvae were homozygous for the *gr* allele, whereas positive VBA-response samples were always *gr siblings (***Fig.3b**).

Furthermore, WISH analysis performed on 5 dpf DMSO and BME treated *gr*$^{+/-}$ incross derived larvae, using *pomca* as probe, showed the presence of upregulated *pomca* expression at the level of the anterior part of the pituitary gland, compared to wild-type siblings (**Fig. 3b'**). Of note, BME treatment was not able to downregulate *pomca* levels of *gr*$^{-/-}$, via negative feedback loop, due to the absence of a functional *gr* allele. Finally, the loss of function was also determined in 5 dpf *gr* mutants by the strong downregulation of *fkbp5* mRNA levels quantified via RTqPCR, both in the presence (fold change=0,01;

P<0,0001) and in the absence of BME treatment (DMSO treated, fold change=0,01; P<0,0001) (**Fig. 3b"**).

gr mutation partially rescues *vhl* phenotype:

We next analyzed the effect of *gr* loss of function on *vhl* phenotype. Phenotypic analysis carried out on 5dpf larvae, derived from $gr^{+/-};vhl^{+/-}$ incross, revealed that *nr3c1* mutation was able to cause an efficient, but not complete rescue of *vhl* phenotype, in a way which resembled *arnt1* mutation (**Fig. 3c**).

In particular, 5dpf $gr^{-/-};vhl^{-/-}$ larvae showed a 43% downregulation at the level of the head (P<0.0001), a 66% downregulation in the liver (P<0.0001) and a 51% downregulation in the tail (from the anus to the caudal peduncle) (P=0.0020), in terms of *phd3::EGFP*-related brightness, compared to $vhl^{-/-}$ larvae (**Fig. 3d and EV3a**). As expected, 5 dpf double mutant larvae were unable to respond to BME [30 μM] treatment (**Fig. 3d and EV3a)**, as also confirmed via RTqPCR analysis on HIF and GCs target genes (**Fig, 3c'**).

Rescue was also apparent by morphology. Indeed, even if $gr^{-/-};vhl^{-/-}$ showed reduced yolk usage, they displayed a reduction in ectopic vessel formation at the level of the dorsal tailfin, no pericardial edema, and developed air-filled swim bladders (**Fig. 3c**). Of note, whereas *vhl* single mutants are inevitably deceased by 10 dpf (van Rooijen *et al.*, 2009), we were able to raise all selected double mutants beyond 15 dpf, but then (similarly to $arnt1^{-/-};vhl^{-/-}$) they failed to grow and thrive when compared to their siblings. This led us to euthanise them due to health concerns at 21 dpf (**Fig. EV3b**). Together, these data indicate for the first time, in our *in vivo* animal model, that GR function is essential to assure a proper HIF response in zebrafish larvae, in particular at the level of the head and the liver.

gr loss of function effect is stronger when HIF-response is attenuated:

The similarity of *gr* and *arnt1* mutations could mean they work in a single linear "pathway". If true, mutation of both should not lead to a further attenuation of the reporter expression. To test this, we bred *gr* in the *arnt1;vhl* double mutant line and we crossed $gr^{+/-};arnt1^{+/-};vhl^{+/-}$ triple mutant carriers. Phenotypic analysis performed on 5 dpf *phd3:eGFP* positive larvae (n=488) showed a small class of larvae with even stronger downregulation of *phd3:eGFP* related brightness, compared to both $arnt1^{-/-};vhl^{-/-}$ and $gr^{-/-};vhl^{-/-}$ double mutants (**Fig. 4a**). Of note, 7 putative very weak GFP^{+} larvae were selected and genotypic analysis confirmed that 5 out of 7 were indeed $gr^{-/-}$; $arnt1^{-/-};vhl^{-/-}$. In

particular, these triple mutants showed a 54% downregulation at the level of the head, a 71% downregulation in the liver and a 72% downregulation in the tail region, in terms of *phd3:eGFP*-related brightness compared to *vhl*$^{-/-}$ (**Fig.4a and EV4**). Thus, these data suggest that GCs are likely to interfere with both Arnt1 and Arnt2 mediated HIF signalling pathway.

BME-induced HIF response is Arnt1 dependent:

To further examine the effect of glucocorticoids on HIF response, we performed BME [30 μM] treatment on all the available mutant lines. As expected, 5 dpf wild-types larvae showed a mild upregulation of *phd3:eGFP*-related brightness at the hepatic level, compared to untreated controls (**Fig.1b and 3d)**. BME treatment was also able to further increase *phd3:eGFP*-related brightness at the level of the head and the liver of 5dpf *vhl*$^{-/-}$, as also confirmed by WISH, using both lactate dehydrogenase A (*ldha*) (**Fig. 5a**) and prolyl hydroxylase 3 (*phd3*) as probes (**Fig. 5b**). As predicted, *gr*$^{-/-}$*;vhl*$^{-/-}$ mutants were unaffected (**Fig.3d**). Interestingly, both *arnt1*$^{-/-}$*;vhl*$^{-/-}$ and *arnt1*$^{-/-}$ *phd3:eGFP*-related brightness was unaffected after BME treatment (**Fig.1c**). RTqPCR analysis carried out on these mutant lines confirmed these data (**Fig.3c'**).

This suggests that in *vhl*$^{-/-}$ larvae, BME treatment can increase HIF response by overriding HIF-mediated *pomca* negative regulation. However, in *arnt1*$^{-/-}$ and *arnt1*$^{-/-}$*;vhl*$^{-/-}$ larvae, even if BME can act downstream of *pomca*, it is not able to trigger HIF response due to *arnt1* loss of function.

***gr* mutation overrides HIF-mediated *pomca* suppression in *gr*$^{-/-}$*;vhl*$^{-/-}$:**

To examine the effect of *gr* loss of function on steroidogenesis in *gr*$^{-/-}$*;vhl*$^{-/-}$, we performed WISH analysis on 5 dpf *gr*$^{+/-}$*;vhl*$^{+/-}$ incross derived larvae, using *pomca* as probe. As expected, *vhl*$^{-/-}$ showed downregulated *pomca* expression, whereas *gr*$^{-/-}$ displayed upregulated *pomca*. Notably, a strong upregulation of *pro-opiomelanocortin a* gene was observed in the double mutants, suggesting that *gr* mutation overrides HIF-mediated *pomca* suppression (**Fig.4b**). PCR-analysis performed post-WISH allowed to determine the presence of genotype-phenotype correlation.

These data suggest that in *gr*$^{-/-}$*;vhl*$^{-/-}$ the uncontrolled upregulation of *pomca*, triggered by *gr* loss of function, cannot be counteracted with the same efficiency by HIF action. Furthermore, even if steroidogenesis is upregulated, endogenous cortisol cannot act via Gr to stimulate the HIF response any longer. Nevertheless, since there is still a

clear upregulation of HIF signaling in *gr*$^{-/-}$;*vhl*$^{-/-}$ larvae compared to wild-types (**Fig.3d**), we considered that the Mr may also able to promote HIF activity.

Both Gr and Mr are directly required for assuring proper HIF response:

Cortisol has high affinity both for Gr and Mr and they have been recently shown to be differentially involved in the regulation of stress axis activation and function in zebrafish (Faught and Vijayan, 2018), Therefore, we analysed the role of *mr* in the HIF response. To achieve this, we knocked-out *mr* in *gr*$^{+/-}$;*vhl*$^{+/-}$;*phd3:eGFP* incrossed derived embryos using CRISPant technology (Wu et al., 2018). Interestingly, phenotypic analysis performed on 5 dpf injected and uninjected larvae revealed that *mr* CRISPR injected *vhl* mutants were characterized by a significant downregulation of *phd3:eGFP*-related brightness at the level of the head (equals to 49%, P<0.0001), in the liver (equals to 56%, P<0.0001) and in the rest of the body (equals to 47%, P<0.0001), compared to *vhl*$^{-/-}$ mutant uninjected larvae (**Fig.6a and 6b**). Moreover, when both *gr* and *mr* were knocked-out, the downregulation was even stronger at the level of the head (equals to 62%, P<0.0001), in the liver (equals to 77%, P<0.0001) and in the rest of the body (equals to 63%, P<0.0001) (**Fig.6a and 6b**).

To confirm the specificity of Wu et al., 2018 method, we chose to target a gene which was not involved in the HIF pathway. *Laminin, beta 1b* (*lamb1b)*, which codes for an extracellular matrix glycoprotein, was injected as CRISPR-injection control in *vhl*$^{+/-}$ incross derived embryos at 1 cell stage. Genotypic analysis carried out on these larvae confirmed that these guides were effective. Finally, quantification of *phd3:eGFP*-related brightness performed on 5 dpf injected and uninjected larvae, showed no significant differences between the two groups (**Fig.6c and 6d**). Overall, these data indicate that both glucocorticoid and mineralocorticoid receptor play a pivotal role in assuring HIF response *in vivo* in zebrafish.

Discussion

HIF and glucocorticoid induced transcriptional responses play a pivotal role in tissue homeostasis, glucose metabolism and in the regulation of cellular responses to various forms of stress and inflammation (Chrousos and Kino, 2009; Revollo and Cidlowski, 2009; Wilson et al., 2016). Previous *in vitro* studies highlighted the potential for cross-talk between HIF and glucocorticoid pathways, however there are still

controversial data on how the interaction between these two major signalling pathways occurs *in vivo*. In this regard, we have presented a novel *in vivo* study using zebrafish larvae, focusing on elucidation of genetic control of one pathway over the other. In contrast to *in vitro* cell culture studies, a whole animal study allows us to take into account the interactions that occur between various tissues and provide novel insights. To do this, we generated *arnt1* and *gr* null mutants to downregulate HIF and GR signalling respectively, as a basis for a genetic analysis of this crosstalk.

Comparison between *arnt1* and *arnt2* in the overall HIF response:

As a prelude to this, we had to establish the relative importance of *arnt1* and *arnt2* in the overall HIF response. To achieve this, a discriminative test was devised to place them in a *vhl* mutant background, where HIF-α is strongly stabilized (van Rooijen *et al.*, 2011; Santhakumar *et al.*, 2012). Phenotypic analysis performed on 5 dpf *arnt1*$^{-/-}$;*vhl*$^{-/-}$ double mutants showed reduced *phd3:eGFP* related brightness, normal yolk usage, properly developed and air-filled swim bladder as well as by the absence of pericardial edema and excessive caudal vasculature. However, beyond 5 days, the double mutants exhibited only partial recovery from the *vhl* phenotype, they developed well till 15 dpf, but subsequently failed to grow and thrive when compared to their siblings. In addition, *arnt1* homozygous mutants were found to be viable and fertile, in contrast to both homozygous *vhl* and *arnt2* mutants, which are embryonic lethal by 8-10 dpf (Hill *et al.*, 2009; van Rooijen *et al.*, 2009).

Of note, the use of a rapid state-of-the-art method aimed to generate CRISPants (Wu *et al.*, 2018) allowed to confirm that Arnt1, even if not fundamental for survival, is predominantly required in the liver and in organs outside the central nervous system for HIF−α function. Conversely, Arnt2 is mainly required in the developing central nervous system (CNS), as also reported by Hill et al. in 2009. However, the similarities observed in terms of *phd3:eGFP*-induced brightness in both *arnt1*$^{-/-}$;*vhl*$^{-/-}$ and *arnt2* CRISPR injected *vhl* mutants, suggests there is no strong functional separation. Therefore, both Arnt2 and Arnt1 have partially overlapping functions *in vivo* and both contribute to the HIF response.

The effect of HIF overexpression on glucocorticoid response:

We next investigated the interplay between HIF and glucocorticoid response, by performing RTqPCR analysis on 5 dpf larvae. Collectively, we show that the presence of

strongly activated (*vhl*$^{-/-}$) and partially attenuated HIF response (*arnt1*$^{-/-}$;*vhl*$^{-/-}$) appears to blunt glucocorticoid signaling, whereas *arnt1* loss of function increased endogenous glucocorticoid response. Furthermore, betamethasone treatment on the aforementioned mutant lines was unable to significantly increase glucocorticoid target genes expression both in *vhl*$^{-/-}$ and in *arnt1*$^{-/-}$;*vhl*$^{-/-}$, whereas it was able to do it in *arnt1*$^{-/-}$ larvae. Together, these results indicate that upregulated HIF levels are somehow able to repress glucocorticoid response and that low normoxic HIF activity nevertheless suffices to attenuate GR activity.

To test whether this was due to any potential effect of overexpressed HIF response on steroidogenesis (Tan *et al.*, 2017), we quantified the expression of steroidogenesis-related genes (*pomca* and *cyp17a2*) both in *vhl*$^{-/-}$ and in *arnt1*$^{-/-}$ larvae, via whole-mount *in situ* hybridization (WISH). Surprisingly, both lines showed downregulation of *pomca*. However, *arnt1*$^{-/-}$ larvae, which were characterized by an upregulated glucocorticoid response, showed upregulated *cyp17a2*, whereas *vhl*$^{-/-}$ larvae, which showed a downregulated GC response, were characterized by downregulated *cyp17a2* expression levels. Consequently, we speculate that in an *arnt1* knock-out scenario, *pomca* downregulation occurs as a consequence of glucocorticoid induced negative feedback loop (aimed to shutdown cortisol biosynthesis). In contrast, as upregulated HIF levels appear to repress *pomca* expression, we speculate that this occurs in a way that resembles the GR-mediated negative feedback loop.

Indeed, as hypoxia represents a potential stressful condition, we speculate that it is initially perceived as a stress by the hypothalamus, which is able to stimulate cortisol biosynthesis and release. In turn, a cortisol-enhanced HIF response activates a series of cellular pro-inflammatory responses aimed to restore homeostasis. As a consequence, to shut down HIF response itself and to avoid an uncontrolled systemic HIF pathway overexpression, HIF might negatively regulate steroidogenesis. Our data would also be in accordance with a previous study that showed that hypoxia exposure resulted in downregulation of steroidogenic genes (*StAR, cyp11c1, hmgcr, hsd17b2, cyp19a, cyp19b*) in 72 hpf larvae, whereas zHIF-α loss of function triggered the upregulation specifically of *StAR*, *cyp11b2* and *cyp17a1* (Tan *et al.*, 2017).

Cumulatively, if this is true, we predicted to observe reduced levels of endogenous glucocorticoids in *vhl*$^{-/-}$ and normal or even increased levels in *arnt1*$^{-/-}$. Indeed, we found that cortisol levels were significantly reduced in *vhl* mutant larvae (where HIF pathway

is overexpressed), whereas they were significantly increased in *arnt1* mutants (where HIF pathway is suppressed).

Together, these data allow us to show the presence of a HIF-induced negative feedback, aimed to blunt steroidogenesis in order to regulate HIF activity itself. By the way, HIF-mediated negative feedback seems to be a logic homeostatic response aimed to avoid a further GCs-induced upregulation of HIF pathway, since hypoxia has been shown to trigger glucocorticoid response (Leonard *et al.*, 2005) and consequently, cortisol was shown to increase HIF expression (Vettori *et al.*, 2017).

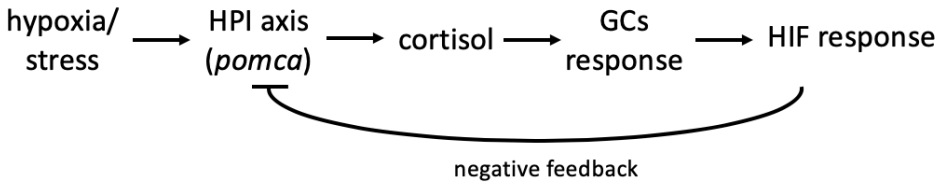

The effect of glucocorticoids on the HIF response:

To investigate the role of glucocorticoids on the HIF response, we initially analyzed the effect of *gr* loss of function on *vhl* phenotype. Surprisingly, we observed that *gr* mutation was able to cause an efficient, but not complete rescue of the *vhl* phenotype, which resembled *arnt1* mutation. Notably, $gr^{-/-};vhl^{-/-}$ survived much longer than $vhl^{-/-}$ (>=21 dpf compared to max. 10 dpf), but then similarly to $arnt1^{-/-};vhl^{-/-}$, they failed to grow and thrive when compared to siblings.

Together, these data indicate for the first time in an *in vivo* animal model that Gr is essential to assure a proper HIF response. Of note, our model based on the negative regulatory effect played by HIF on *pomca* expression, may provide a reliable explanation of this phenotype. In particular, we speculate that in $gr^{-/-};vhl^{-/-}$, the absence of GC-GR negative feedback loop triggers a strong upregulation of *pomca* (**Fig.4b**), which cannot be counteracted with the same efficiency by upregulated HIF levels (via HIF-mediated negative feedback). In this scenario, the elevated endogenous cortisol levels cannot interact with Gr any longer. Consequently, since cortisol acts via glucocorticoid receptor as an enhancer of the HIF response (Kodama *et al.*, 2003; Vettori Andrea *et al.*, 2016), *gr* loss of function results in an attenuated HIF pathway activation.

If this is true, we predicted to obtain an even more rescued phenotype by knocking-out *gr* in an attenuated HIF scenario. Phenotypic analysis performed on $gr^{+/-};arnt1^{+/-};vhl^{-/-};phd3:EGFP$ triple mutant line confirmed this. To further examine the role of

glucocorticoids on HIF response, we next analysed the effect of betamethasone treatment on *gr*$^{-/-}$*;vhl*$^{-/-}$*;phd3:eGFP, arnt1*$^{-/-}$*;phd3:eGFP* and *arnt1*$^{-/-}$*;vhl*$^{-/-}$*;phd3:eGFP* mutants. Our results indicate a key role for Arnt1 in regulating BME-induced HIF response. This is evident by the lack of *phd3:eGFP*-related brightness increase observed both in *arnt1*$^{-/-}$ and in *arnt1*$^{-/-}$*;vhl*$^{-/-}$ larvae, after BME administration.

Cumulatively, we suggest that HIF-mediated negative feedback on *pomca* expression can occur both via Arnt1 and Arnt2, whilst BME-induced HIF upregulation mainly requires functional Arnt1.

Evaluation of mineralocorticoid receptor contribution to HIF response:

Previous work published by Faught and Vijayan, 2018 showed that both Gr and Mr are differentially involved in the regulation of zebrafish stress axis activation and function. In addition, our results suggest that both glucocorticoids and Gr exert a pivotal role in the HIF response. Since nothing was known about mineralocorticoid receptor contribution to the HIF response, we tested the effect of *mr* knock-out in *gr*$^{+/-}$*;vhl*$^{+/-}$*;phd3:EGFP* incrossed derived embryos. Both in *mr* injected- *vhl*$^{-/-}$ and *gr*$^{-/-}$*;vhl*$^{-/-}$ 5 dpf larvae, we showed a significant reduction of *phd3:eGFP*-related brightness. These data suggest that in fish not only the glucocorticoid receptor, but also the mineralocorticoid receptor is involved in promoting HIF pathway activation, as a consequence of cortisol stimulation. Indeed, in contrast to mammals, teleosts lack aldosterone and cortisol is the primary glucocorticoid hormone which can interact with both Gr and Mr to assure the correct HPI axis functioning (Cruz *et al.*, 2013; Baker and Katsu, 2017). Of note, our hypothesis is supported by Faught and Vijayan, 2018 recent work, showing that both Gr and Mr signalling is involved in the negative feedback regulation of cortisol biosynthesis during stress.

In conclusion, although Mr contribution to HIF response in other organisms remains unclear, our work suggests research into its function is warranted.

Conclusion

Our present study stresses the importance of the glucocorticoid pathway in driving HIF response. In addition, we uncovered a negative regulatory role played by overexpression of HIF in regulating steroidogenesis as demonstrated via RTqPCR and steroid hormone quantification. We also report a novel key role for Arnt1 in regulating

BME-induced HIF response and identify a possible mineralocorticoid receptor contribution to HIF-GC crosstalk. Finally, we presented novel *gr*$^{+/-}$*;vhl*$^{+/-}$, *arnt1*$^{+/-}$*;vhl*$^{+/-}$ and *arnt1*$^{+/-}$*;gr*$^{+/-}$*;vhl*$^{+/-}$ zebrafish mutant lines which helped to better understand how the interplay between HIF and glucocorticoids occur *in vivo*. For these reasons, we believe that this work could pave the way for further *in vivo* analysis to precisely identify the extensive crosstalk behind these two major signalling pathways.

Data availability

All data are available on request.

Author contribution

Financial support: BB/R015457/1; BB/M02332X/1, TUoS; Investigation, validation and data curation: DM, FVE; Formal visualization and analysis: DM; Resources: FVE, EM, KS, NL, HE, VTC, NK; Project Administration: DM, FVE; Writing-Original Draft: DM and FVE; Writing -Review and Editing: all authors contributed equally.

Conflict of interest

The authors declare that they have no conflict of interest.

Acknowledgements

We thank the University of Sheffield aquarium staff for the excellent care of fish stocks. We are grateful to Rosemary Kim, Helen Eachus, Emily Noël, Chris Derrick, Jack Paveley and Dheemanth Subramanya for useful discussions contributing to this study and for sharing chemical compounds. We also thank Elisabeth Kugler for her technical support for image analysis. This work was supported by a University of Sheffield, Biomedical Science department studentship awarded by DM and by two BBRSC grants to FVE (BB/R015457/1; BB/M02332X/1). N.K was funded by the Deutsche Forschungs grant (KR3363/3-1).

References

1. Alsop, D. and Vijayan, M. (2009) 'The zebrafish stress axis: Molecular fallout from the teleost-specific genome duplication event', *General and Comparative Endocrinology*. Elsevier Inc., 161(1), pp. 62–66. doi: 10.1016/j.ygcen.2008.09.011.
2. Alsop, D. and Vijayan, M. M. (2008) 'Development of the corticosteroid stress axis and receptor expression in zebrafish.', *American journal of physiology. Regulatory, integrative and comparative physiology*, 294(3), pp. R711–R719. doi: 10.1152/ajpregu.00671.2007.
3. Baker, M. E. and Katsu, Y. (2017) '30 YEARS OF THE MINERALOCORTICOID RECEPTOR: Evolution of the mineralocorticoid receptor: sequence, structure and function', *Journal of Endocrinology*. Bristol, UK: Bioscientifica Ltd, 234(1), pp. T1–T16. doi: 10.1530/JOE-16-0661.
4. Bamberger, C. M., Schulte, H. M. and Chrousos, G. P. (1996) 'Molecular Determinants of Glucocorticoid Receptor Function and Tissue Sensitivity to Glucocorticoids', *Endocrine Reviews*, 17(3), pp. 245–261. doi: 10.1210/edrv-17-3-245.
5. Barnes, P. J. (2011) 'Glucocorticosteroids: current and future directions', *British Journal of Pharmacology*. John Wiley & Sons, Ltd (10.1111), 163(1), pp. 29–43. doi: 10.1111/j.1476-5381.2010.01199.x.
6. Barnes, P. J. and Adcock, I. M. (2009) 'Glucocorticoid resistance in inflammatory diseases', *The Lancet*. Elsevier, 373(9678), pp. 1905–1917. doi: 10.1016/S0140-6736(09)60326-3.
7. Bertout, J. A., Patel, S. A. and Simon, M. C. (2008) 'The impact of O2 availability on human cancer.', *Nature reviews. Cancer*, 8(12), pp. 967–75. doi: 10.1038/nrc2540.
8. Busillo, J. M. and Cidlowski, J. A. (2013) 'The five Rs of glucocorticoid action during inflammation: Ready, reinforce, repress, resolve, and restore', *Trends in Endocrinology and Metabolism*. doi: 10.1016/j.tem.2012.11.005.
9. Chatzopoulou, A. *et al.* (2015) 'Transcriptional and metabolic effects of glucocorticoid receptor α and β signaling in zebrafish', *Endocrinology*, 156(5), pp. 1757–1769. doi: 10.1210/en.2014-1941.
10. Cruz, S. A. *et al.* (2013) 'Glucocorticoid Receptor, but Not Mineralocorticoid Receptor, Mediates Cortisol Regulation of Epidermal Ionocyte Development and Ion Transport in Zebrafish (Danio Rerio)', *PLOS ONE*. Public Library of Science, 8(10), p. e77997. Available at: https://doi.org/10.1371/journal.pone.0077997.

11. Cummins, E. P. and Taylor, C. T. (2005) 'Hypoxia-responsive transcription factors', *Pflugers Archiv European Journal of Physiology*, 450(6), pp. 363–371. doi: 10.1007/s00424-005-1413-7.
12. Dittrich, A. *et al.* (2012) 'Glucocorticoids increase interleukin-6–dependent gene induction by interfering with the expression of the suppressor of cytokine signaling 3 feedback inhibitor', *Hepatology*. John Wiley & Sons, Ltd, 55(1), pp. 256–266. doi: 10.1002/hep.24655.
13. Eachus, H. *et al.* (2017) 'Genetic disruption of 21-hydroxylase in zebrafish causes interrenal hyperplasia', *Endocrinology*, 158(12), pp. 4165–4173. doi: 10.1210/en.2017-00549.
14. Elks, P. M. *et al.* (2015) 'Exploring the HIFs, buts and maybes of hypoxia signalling in disease: lessons from zebrafish models.', *Disease models & mechanisms*, 8(11), pp. 1349–60. doi: 10.1242/dmm.021865.
15. Facchinello, N. *et al.* (2017) 'nr3c1 null mutant zebrafish are viable and reveal DNA-binding-independent activities of the glucocorticoid receptor', *Scientific Reports*. London: Nature Publishing Group UK, 7, p. 4371. doi: 10.1038/s41598-017-04535-6.
16. Faught, E. and Vijayan, M. M. (2018) 'The mineralocorticoid receptor is essential for stress axis regulation in zebrafish larvae', *Scientific Reports*. Springer US, 8(1), pp. 1–11. doi: 10.1038/s41598-018-36681-w.
17. Gaber, T. *et al.* (2011) 'Macrophage Migration Inhibitory Factor Counterregulates Dexamethasone-Mediated Suppression of Hypoxia-Inducible Factor-1α Function and Differentially Influences Human CD4⁺ T Cell Proliferation under Hypoxia', *The Journal of Immunology*, 186(2), pp. 764 LP – 774. doi: 10.4049/jimmunol.0903421.
18. Griffiths, B. B. *et al.* (2012) 'A zebrafish model of glucocorticoid resistance shows serotonergic modulation of the stress response.', *Frontiers in behavioral neuroscience*, 6(October), p. 68. doi: 10.3389/fnbeh.2012.00068.
19. Hatamoto, K. and Shingyoji, C. (2008) 'Cyclical training enhances the melanophore responses of zebrafish to background colours', *Pigment Cell & Melanoma Research*. John Wiley & Sons, Ltd (10.1111), 21(3), pp. 397–406. doi: 10.1111/j.1755-148X.2008.00445.x.
20. Hill, A. J. *et al.* (2009) 'Potential Roles of Arnt2 in Zebrafish Larval Development', *Zebrafish*. 140 Huguenot Street, 3rd FloorNew Rochelle, NY 10801USA: Mary Ann

Liebert, Inc., 6(1), pp. 79–91. doi: 10.1089/zeb.2008.0536.

21. Hruscha, A. *et al.* (2013) 'Efficient CRISPR/Cas9 genome editing with low off-target effects in zebrafish', *Development*, 140(May), pp. 4982–4987. doi: 10.1242/dev.099085.
22. Kimmel, C. B. *et al.* (1995) 'Stages of Embryonic Development of the Zebrafish', *Developmental Dynamics*, 203, pp. 253–310. doi: 10.1002/aja.1002030302.
23. Kodama, T. *et al.* (2003) 'Role of the glucocorticoid receptor for regulation of hypoxia-dependent gene expression', *Journal of Biological Chemistry*, 278(35), pp. 33384–33391. doi: 10.1074/jbc.M302581200.
24. Kong *et al.* (2017) 'Overexpression and Knockdown of Hypoxia-Inducible Factor 1 Disrupt the Expression of Steroidogenic Enzyme Genes and Early Embryonic Development in Zebrafish', *Gene Regulation and Systems Biology*, 11(0). doi: 10.1177/1177625017713193.
25. Kramer, B. M. R. *et al.* (2001) 'Dynamics and plasticity of peptidergic control centres in the retino-brain-pituitary system of Xenopus laevis', *Microscopy Research and Technique*. John Wiley & Sons, Ltd, 54(3), pp. 188–199. doi: 10.1002/jemt.1132.
26. Kurrasch, D. M. *et al.* (2009) 'Neuroendocrine transcriptional programs adapt dynamically to the supply and demand for neuropeptides as revealed in NSF mutant zebrafish', *Neural development*. BioMed Central, 4, p. 22. doi: 10.1186/1749-8104-4-22.
27. Labun, K. *et al.* (2016) 'CHOPCHOP v2: a web tool for the next generation of CRISPR genome engineering', *Nucleic Acids Research*, 44(W1), pp. W272–W276. doi: 10.1093/nar/gkw398.
28. Langlais, D. *et al.* (2008) 'Regulatory Network Analyses Reveal Genome-Wide Potentiation of LIF Signaling by Glucocorticoids and Define an Innate Cell Defense Response', *PLOS Genetics*. Public Library of Science, 4(10), p. e1000224. Available at: https://doi.org/10.1371/journal.pgen.1000224.
29. Langlais, D. *et al.* (2012) 'The Stat3/GR Interaction Code: Predictive Value of Direct/Indirect DNA Recruitment for Transcription Outcome', *Molecular Cell*. Cell Press, 47(1), pp. 38–49. doi: 10.1016/J.MOLCEL.2012.04.021.
30. Leonard, M. O. *et al.* (2005) 'Potentiation of Glucocorticoid Activity in Hypoxia through Induction of the Glucocorticoid Receptor', *The Journal of Immunology*, 174, pp. 2250–2257. doi: 10.4049/jimmunol.174.4.2250.
31. Livak, K. J. and Schmittgen, T. D. (2001) 'Analysis of Relative Gene Expression Data

Using Real-Time Quantitative PCR and the 2−ΔΔCT Method', *Methods*. Academic Press, 25(4), pp. 402–408. doi: 10.1006/METH.2001.1262.

32. Mitre-Aguilar, I. B., Cabrera-Quintero, A. J. and Zentella-Dehesa, A. (2015) 'Genomic and non-genomic effects of glucocorticoids: implications for breast cancer', *International journal of clinical and experimental pathology*. e-Century Publishing Corporation, 8(1), pp. 1–10. Available at: https://www.ncbi.nlm.nih.gov/pubmed/25755688.
33. Moghadam-Kia, S. and Werth, V. P. (2010) 'Prevention and treatment of systemic glucocorticoid side effects', *International Journal of Dermatology*. John Wiley & Sons, Ltd (10.1111), 49(3), pp. 239–248. doi: 10.1111/j.1365-4632.2009.04322.x.
34. Montague, T. G. *et al.* (2014) 'CHOPCHOP: a CRISPR/Cas9 and TALEN web tool for genome editing', *Nucleic acids research*. 2014/05/26. Oxford University Press, 42(Web Server issue), pp. W401–W407. doi: 10.1093/nar/gku410.
35. Muthu, V. *et al.* (2016) 'Rx3 and Shh direct anisotropic growth and specification in the zebrafish tuberal/anterior hypothalamus', *Development*, 143(14), pp. 2651 LP – 2663. doi: 10.1242/dev.138305.
36. Muto, A. *et al.* (2005) 'Forward Genetic Analysis of Visual Behavior in Zebrafish', *PLOS Genetics*. Public Library of Science, 1(5), p. e66. Available at: https://doi.org/10.1371/journal.pgen.0010066.
37. Muto, A. *et al.* (2013) 'Glucocorticoid receptor activity regulates light adaptation in the zebrafish retina.', *Frontiers in neural circuits*, 7(September), p. 145. doi: 10.3389/fncir.2013.00145.
38. Neeck, G., Renkawitz, R. and Eggert, M. (2002) 'Molecular aspects of glucocorticoid hormone action in rheumatoid arthritis', *Cytokines, Cellular & Molecular Therapy*, 7(2), pp. 61–69. doi: 10.1080/13684730412331302081.
39. Nikolaus, S., Fölscn, U. and Schreiber, S. (2000) *Immunopharmacology of 5-aminosalicylic acid and of glucocorticoids in the therapy of inflammatory bowel disease*, *Hepato-gastroenterology*.
40. Panettieri, R. A. *et al.* (2019) 'Non-genomic Effects of Glucocorticoids: An Updated View', *Trends in Pharmacological Sciences*. doi: 10.1016/j.tips.2018.11.002.
41. Pescador, N. *et al.* (2005) 'Identification of a functional hypoxia-responsive element that regulates the expression of the egl nine homologue 3 (egln3/phd3) gene', *The Biochemical journal*. Portland Press Ltd., 390(Pt 1), pp. 189–197. doi: 10.1042/BJ20042121.

42. Ramamoorthy, S. and Cidlowski, J. A. (2016) 'Corticosteroids. Mechanisms of Action in Health and Disease', *Rheumatic Disease Clinics of North America*. doi: 10.1016/j.rdc.2015.08.002.
43. van Rooijen, E. *et al.* (2009) 'Zebrafish mutants in the von Hippel-Lindau tumor suppressor display a hypoxic response and recapitulate key aspects of Chuvash polycythemia', *Blood*, 113(25), pp. 6449 LP – 6460. doi: 10.1182/blood-2008-07-167890.
44. van Rooijen, E. *et al.* (2011) 'A Zebrafish Model for VHL and Hypoxia Signaling', *Methods in Cell Biology*, 105(December 2011), pp. 163–190. doi: 10.1016/B978-0-12-381320-6.00007-2.
45. Rooijen, E. Van *et al.* (2009) 'Zebrafish mutants in the von Hippel-Lindau (VHL) tumor suppressor display a hypoxic response and recapitulate key aspects of Chuvash polycythemia Hubrecht Institute - KNAW & University Medical Center Utrecht , The Netherlands * R . H . G and F . J . V .', *Hematology*, 113(25), pp. 6449–6461. doi: 10.1182/blood-2008-07-167890.
46. Santhakumar, K. *et al.* (2012) 'A zebrafish model to study and therapeutically manipulate hypoxia signaling in tumorigenesis', *Cancer Research*, 72(16), pp. 4017–4027. doi: 10.1158/0008-5472.CAN-11-3148.
47. Semenza, G. L. (2011) 'Oxygen Sensing, Homeostasis, and Disease', *New England Journal of Medicine*. Massachusetts Medical Society, 365(6), pp. 537–547. doi: 10.1056/NEJMra1011165.
48. Semenza, G. L. (2012) 'Hypoxia-inducible factors in physiology and medicine', *Cell*, 148(3), pp. 399–408. doi: 10.1016/j.cell.2012.01.021.
49. Semenza, G. L. (2013) 'HIF-1 mediates metabolic responses to intratumoral hypoxia and oncogenic mutations', *Journal of Clinical Investigation*, 123(9), pp. 3664–3671. doi: 10.1172/JCI67230.
50. Stahn, C. and Buttgereit, F. (2008) 'Genomic and nongenomic effects of glucocorticoids', *Nature Clinical Practice Rheumatology*. Nature Publishing Group, 4, p. 525. Available at: https://doi.org/10.1038/ncprheum0898.
51. Tan, T. *et al.* (2017) 'Overexpression and Knockdown of Hypoxia-Inducible Factor 1 Disrupt the Expression of Steroidogenic Enzyme Genes and Early Embryonic Development in Zebrafish', *Gene regulation and systems biology*. SAGE Publications, 11,pp.1177625017713193–1177625017713193.doi:10.1177/1177625017713193.
52. Thisse, C. and Thisse, B. (2008) 'High-resolution in situ hybridization to whole-mount

zebrafish embryos', *Nature Protocols*. Nature Publishing Group, 3, p. 59. Available at: https://doi.org/10.1038/nprot.2007.514.

53. Tokarz, J. *et al.* (2013) 'Zebrafish and steroids: What do we know and what do we need to know?', *Journal of Steroid Biochemistry and Molecular Biology*. doi: 10.1016/j.jsbmb.2013.01.003.
54. Vettori, A. *et al.* (2017) 'Glucocorticoids promote Von Hippel Lindau degradation and Hif-1α stabilization', *Proceedings of the National Academy of Sciences*, p. 201705338. doi: 10.1073/pnas.1705338114.
55. Wagner, A. E. *et al.* (2008) 'Dexamethasone impairs hypoxia-inducible factor-1 function', *Biochemical and Biophysical Research Communications*, 372(2), pp. 336–340. doi: 10.1016/j.bbrc.2008.05.061.
56. Weger, B. D. *et al.* (2016) 'Extensive Regulation of Diurnal Transcription and Metabolism by Glucocorticoids', *PLOS Genetics*. Public Library of Science, 12(12), p. e1006512. Available at: https://doi.org/10.1371/journal.pgen.1006512.
57. Weger, M. *et al.* (2018) 'Expression and activity profiling of the steroidogenic enzymes of glucocorticoid biosynthesis and the fdx1 co-factors in zebrafish', *Journal of Neuroendocrinology*, 30(4), pp. 1–15. doi: 10.1111/jne.12586.
58. Wu, R. S. *et al.* (2018) 'A Rapid Method for Directed Gene Knockout for Screening in G0 Zebrafish', *Developmental Cell*. Elsevier Inc., 46(1), pp. 112-125.e4. doi: 10.1016/j.devcel.2018.06.003.
59. Xie, Y. *et al.* (2019) 'Glucocorticoids inhibit macrophage differentiation towards a pro-inflammatory phenotype upon wounding without affecting their migration', *bioRxiv*, p. 473926. doi: 10.1101/473926.
60. Zhang, C. *et al.* (2015) 'Effects of hypoxia inducible factor-1α on apoptotic inhibition and glucocorticoid receptor downregulation by dexamethasone in AtT-20 cells', *BMC Endocrine Disorders*. BMC Endocrine Disorders, 15(24), pp. 1–9. doi: 10.1186/s12902-015-0017-2.
61. Zhang, H. *et al.* (2011) 'Hypoxia-Inducible Factor Directs POMC Gene to Mediate Hypothalamic Glucose Sensing and Energy Balance Regulation', *PLOS Biology*. Public Library of Science, 9(7), p. e1001112. Available at: https://doi.org/10.1371/journal.pbio.1001112.
62. Zhang, P. *et al.* (2016) 'Down-regulation of GR?? expression and inhibition of its nuclear translocation by hypoxia', *Life Sciences*, 146, pp. 92–99. doi: 10.1016/j.lfs.2015.12.059.

63. Ziv, L. *et al.* (2012) 'An affective disorder in zebrafish with mutation of the glucocorticoid receptor', *Molecular Psychiatry*. Nature Publishing Group, 18(6), pp. 681–691. doi: 10.1038/mp.2012.64.

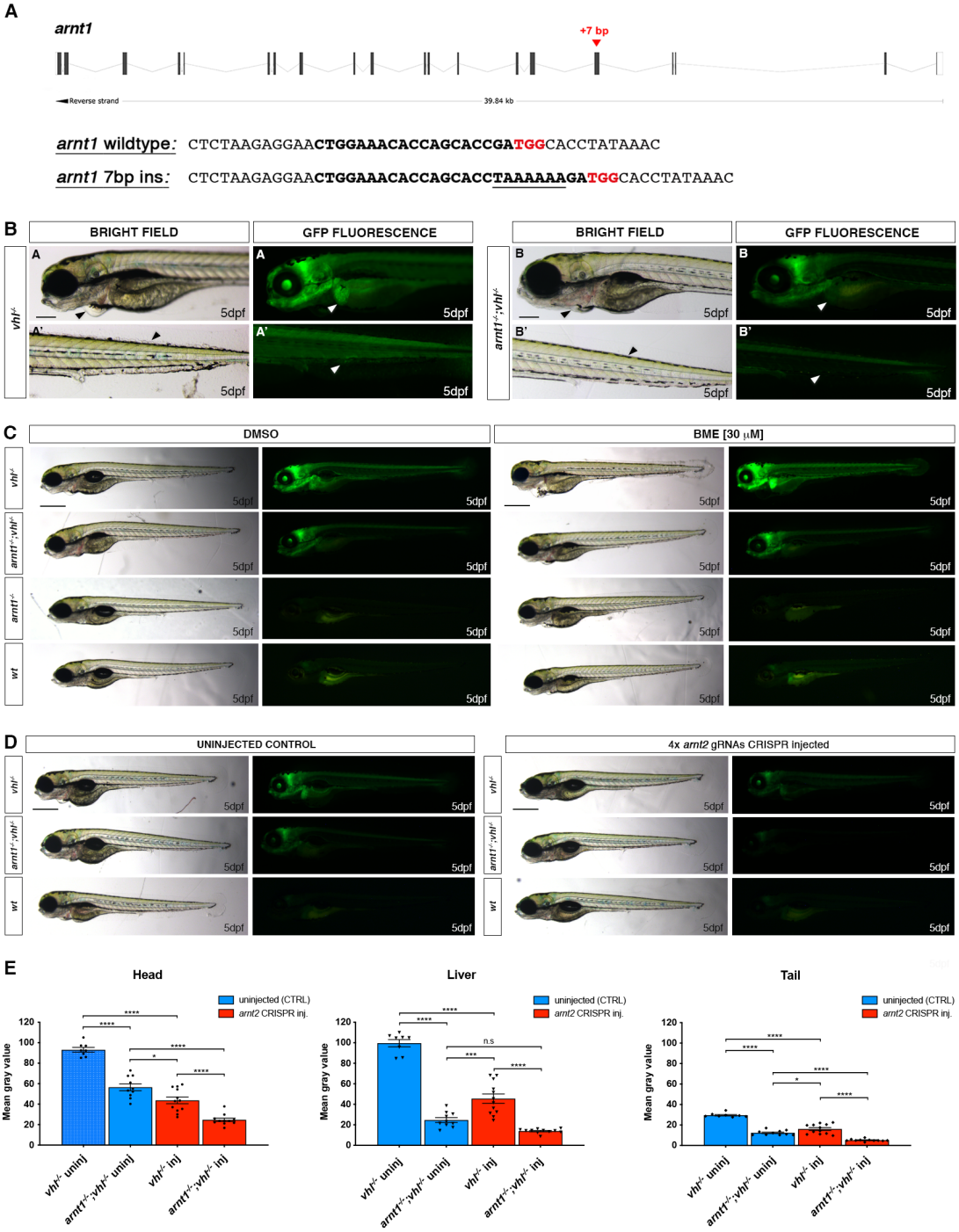

Figure 1. *arnt1* and *arnt2* has partially overlapping functions and synergistically contribute to HIF response.

A. Schematic representation of zebrafish *hif1β* (*arnt1*) gene. Exons are shown as black boxes, whereas introns as lines. The red arrowhead shows the position of a +7 bp insertion in exon 5 (encoding the bHLH DNA binding domain). In the *arnt1* wt and mutant sequence. CRISPR target site: bold. Protospacer-adjacent-motif (PAM) sequence: red.

B. Magnified picture of a representative 5 dpf *vhl*$^{-/-}$ larva compared to 5dpf *arnt1*$^{-/-}$;*vhl*$^{-/-}$. Among the 120 GFP^{+} embryos derived from *arnt1*$^{+/-}$;*vhl*$^{+/-}$(*phd3:eGFP*) x *arnt1*$^{-/-}$;*vhl*$^{+/-}$(*phd3:eGFP*), 15 larvae were characterized by the absence of pericardial oedema, no ectopic extra vasculature at the level of the tail, no bright liver and a reduced brightness in the rest of the body (black and white arrowheads). Genotyping post phenotypic analysis on sorted larvae confirmed genotype-phenotype correlation. Fluorescence, exposure = 2 seconds. Scale bar 200 μm.

C. Representative picture of phenotypic analysis performed on DMSO and BME [30 μM] treated 5 dpf larvae, derived from *arnt1*$^{+/-}$;*vhl*$^{+/-}$(*phd3:eGFP*) x *arnt1*$^{-/-}$;*vhl*$^{+/-}$(*phd3:eGFP*) (n=540). Among the 405 GFP^{+} larvae, all the 25 *arnt1*$^{-/-}$;*vhl*$^{-/-}$ showed the aforementioned partially rescued vhl phenotype (B). Fluorescence, exposure = 2 seconds. Scale bar 500 μm.

D. Representative pictures of 5 dpf CRISPANT mutants created by redundantly targeting *arnt2* gene via co-injection of 4x gRNAs in *arnt1*$^{+/-}$;*vhl*$^{+/-}$(*phd3:eGFP*) x *arnt1*$^{-/-}$; *vhl*$^{+/-}$(*phd3:eGFP*) derived embryos (n=300). Uninjected embryos were used as control (n=120). Fluorescence, exposure = 991,4 ms. Scale bar 500 μm.

E. Statistical analysis performed on mean grey values quantification (at the level of the head, liver and tail), after phenotypic analysis on 5 dpf *arnt2* 4x gRNAs injected and uninjected larvae. *vhl*$^{-/-}$ uninjected n = 8 larvae: head 93.1 ± 2.33 (mean ± s.e.m); liver 99.65 ± 3.49 (mean ± s.e.m); tail 29.58 ± 0.73 (mean ± s.e.m). *arnt1*$^{-/-}$;*vhl*$^{-/-}$ uninjected n = 10 larvae: head 56.49 ± 3.36 (mean ± s.e.m); liver 24,7 ± 2.36 (mean ± s.e.m); tail 12.39 ± 0,75 (mean ± s.e.m). *vhl*$^{-/-}$ injected n = 12 larvae: head 43.69 ± 3.25 (mean ± s.e.m); liver 45.54 ± 4.57 (mean ± s.e.m); tail 16.09 ± 1.37 (mean ± s.e.m). *arnt1*$^{-/-}$;*vhl*$^{-/-}$ injected n = 11 larvae: head 24.66 ± 1.63 (mean ± s.e.m); liver 13.88 ± 0.66 (mean ± s.e.m); tail 5.16 ± 0.33 (mean ± s.e.m). Ordinary One-way ANOVA followed by Sidak's multiple comparison test (*P < 0.05; **P < 0.01; ***P <0.001; ****P < 0.0001).

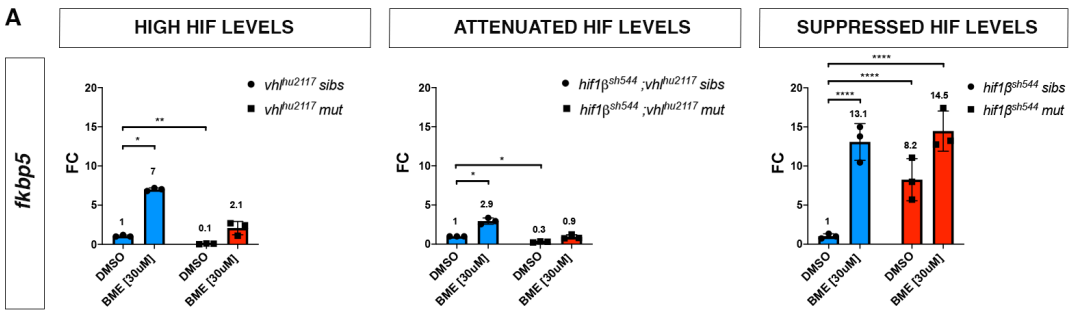

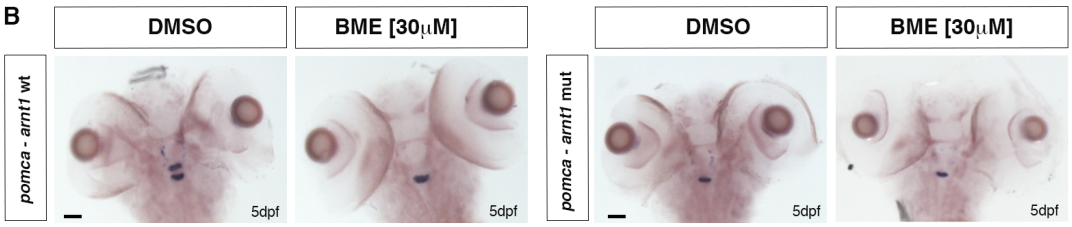

B' *arnt1*$^{-/-}$ ⊣ suppressed HIF → GCs response → **GC-GR negative feedback** ⊣ *pomca*

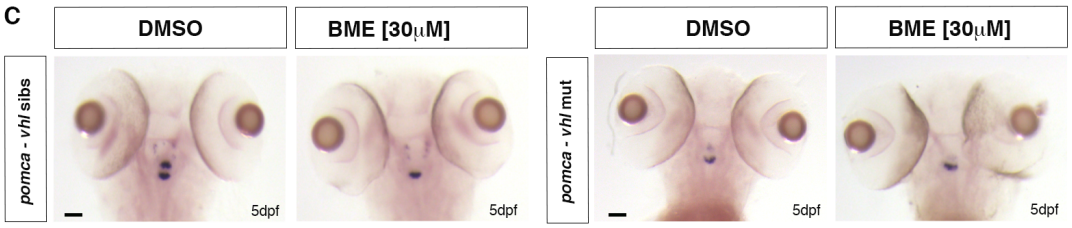

C' *vhl*$^{-/-}$ → upregulated HIF → **HIF negative feedback?** ⊣ *pomca* ⊣ GCs response

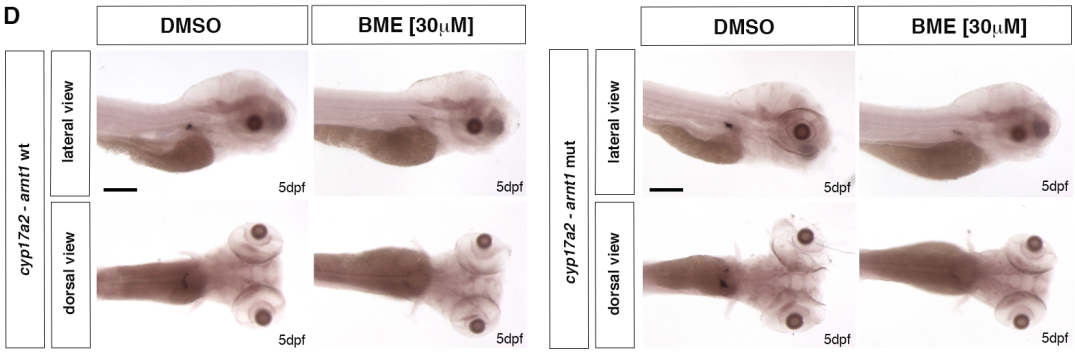

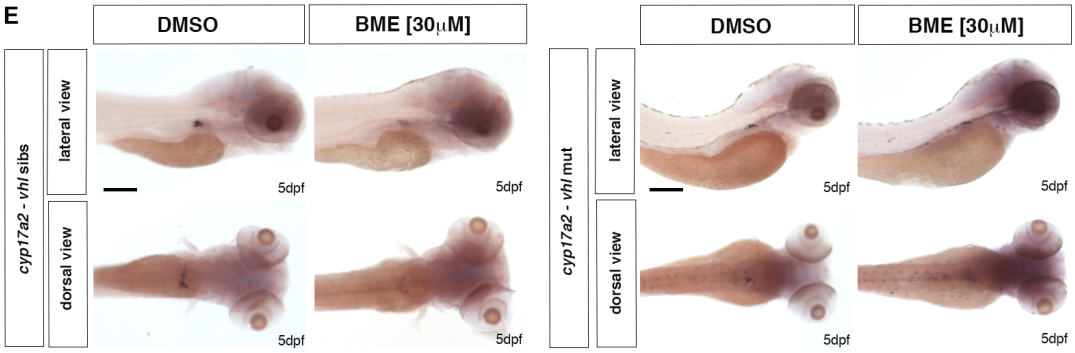

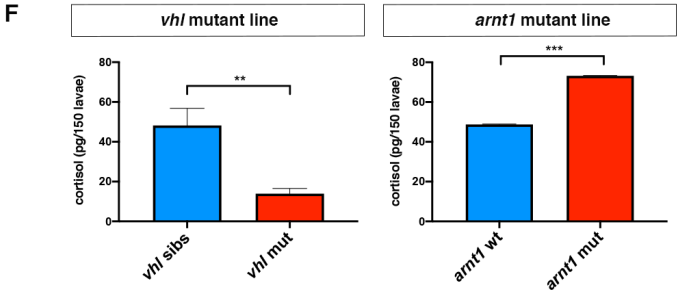

Figure 2. HIF levels inversely correlate with GC response and cortisol biosynthesis.

A. Schematic view of RTqPCR analysis on *fkbp5* expression performed on the following mutant lines at 5 dpf: *vhl*$^{+/-}$*(phd3:eGFP), arnt1*$^{+/-}$*;vhl*$^{+/-}$*(phd3:eGFP)* and *arnt1*$^{+/-}$*(phd3:eGFP).* Upregulated (in *vhl*$^{-/-}$) and attenuated high (in *arnt1*$^{-/-}$*;vhl*$^{-/-}$) HIF levels downregulate GC response, whereas *arnt1* loss of function sensitises larvae to glucocorticoids. Statistical analysis was performed on ΔΔCt values, whereas data are shown as fold change values for RTqPCR analysed samples; ordinary Two-way ANOVA followed by Dunnett's multiple comparison test (*P < 0.05; **P < 0.01; ***P <0.001; ****P < 0.0001).

B. Representative pictures of WISH performed on DMSO and BME [30 μM] treated *arnt1* mutant line, at 5 dpf, using *pomca* as probe. *arnt1* wt DMSO treated (n= 30/30 larvae) showed normal pomca expression; *arnt1* wt BME treated (n= 29/30 larvae) showed downregulated pomca expression. In contrast, *arnt1*$^{-/-}$ DMSO treated (n= 28/30) and *arnt1*$^{-/-}$ BME treated (n= 30/30) larvae showed downregulated pomca expression. Chi-square test (****P < 0.0001). Scale bar 50 μm.

B'. Representative scheme of the putative effect of downregulated HIF levels on GC response. In the presence of *arnt1* loss of function, *pomca* expression is downregulated. We speculate that this is due to the upregulated GC response, as previously shown by RTqPCR analysis, which triggers the GC-GR negative feedback loop in *arnt1*$^{-/-}$ larvae.

C. Representative pictures of WISH performed on DMSO and BME [30 μM] treated *vhl* mutant line, at 5 dpf, using *pomca* as probe. DMSO treated *vhl* siblings (n= 26/28) showed normal *pomca* expression; BME treated *vhl* siblings (n= 28/30) showed downregulated *pomca* expression. In contrast, *vhl*$^{-/-}$ DMSO (n= 28/29) and BME (n= 28/28) treated larvae showed downregulated *pomca* expression. Chi-square test (****P < 0.0001). Scale bar 50 μm.

C'. Representative scheme of the putative effect of upregulated HIF levels on GC response. In the presence of high HIF levels, *pomca* expression is downregulated. We hypothesize that this due to a specific HIF-mediated negative effect on *pomca* expression, which in turn results in the downregulated GC response observed in *vhl*$^{-/-}$ larvae, as also shown by RTqPCR analysis.

D. Representative pictures of WISH performed on DMSO and BME [30 μM] treated *arnt1* mutant line, at 5 dpf, using *cyp17a2* as probe. *arnt1* wt DMSO treated larvae (n= 26/28) showed normal *cyp17a2* expression, whereas 2/28 larvae showed a weaker one; *arnt1* wt BME treated larvae (n= 28/30) showed downregulated *cyp17a2* expression, whereas 2/30 larvae showed a normal one. In contrast, *arnt1*$^{-/-}$ DMSO treated larvae (n= 24/28) showed upregulated *cyp17a2* expression, whereas 4/28 larvae showed a weaker *one. arnt1*$^{-/-}$ BME treated larvae (n= 25/29) showed downregulated *cyp17a2* expression, whereas 4/29, showed a normal one. Chi-square test (****P < 0.0001). Scale bar 200 μm.

E. Representative pictures of WISH performed on DMSO and BME [30 μM] treated *vhl* mutant line, at 5 dpf, using *cyp17a2* as probe. DMSO treated *vhl* siblings (n= 18/21) showed normal *cyp17a2* expression, whereas 3/21 larvae showed a weaker one; BME treated *vhl* siblings (n= 28/30) showed downregulated *cyp17a2* expression, whereas 2/30 larvae showed a normal one. On the other hand, *arnt1*$^{-/-}$ DMSO treated larvae (n= 27/28) showed weak *cyp17a2* expression, whereas 1/28 larvae showed a normal *one. arnt1*$^{-/-}$ BME treated larvae (n= 30/30) showed downregulated *cyp17a2* expression. Chi-square test (****P < 0.0001). Scale bar 200 μm.

F. Steroid quantification results showed a significantly reduced cortisol concentration (P value <0;0028) in *vhl* mutants (13.9 pg/150 larvae, in triplicate), compared to *vhl* siblings (48.2 pg/150 larvae, in triplicate) at 5 dpf. Moreover, a significantly increased cortisol concentration (P value <0;0001) was measured in *arnt1* mutants (66.8 pg/150 larvae, in triplicate), compared to *arnt1* wild-types (48.7 pg/150 larvae, in triplicate) at 5 dpf; unpaired t-test (**P < 0.01; ***P <0.001).

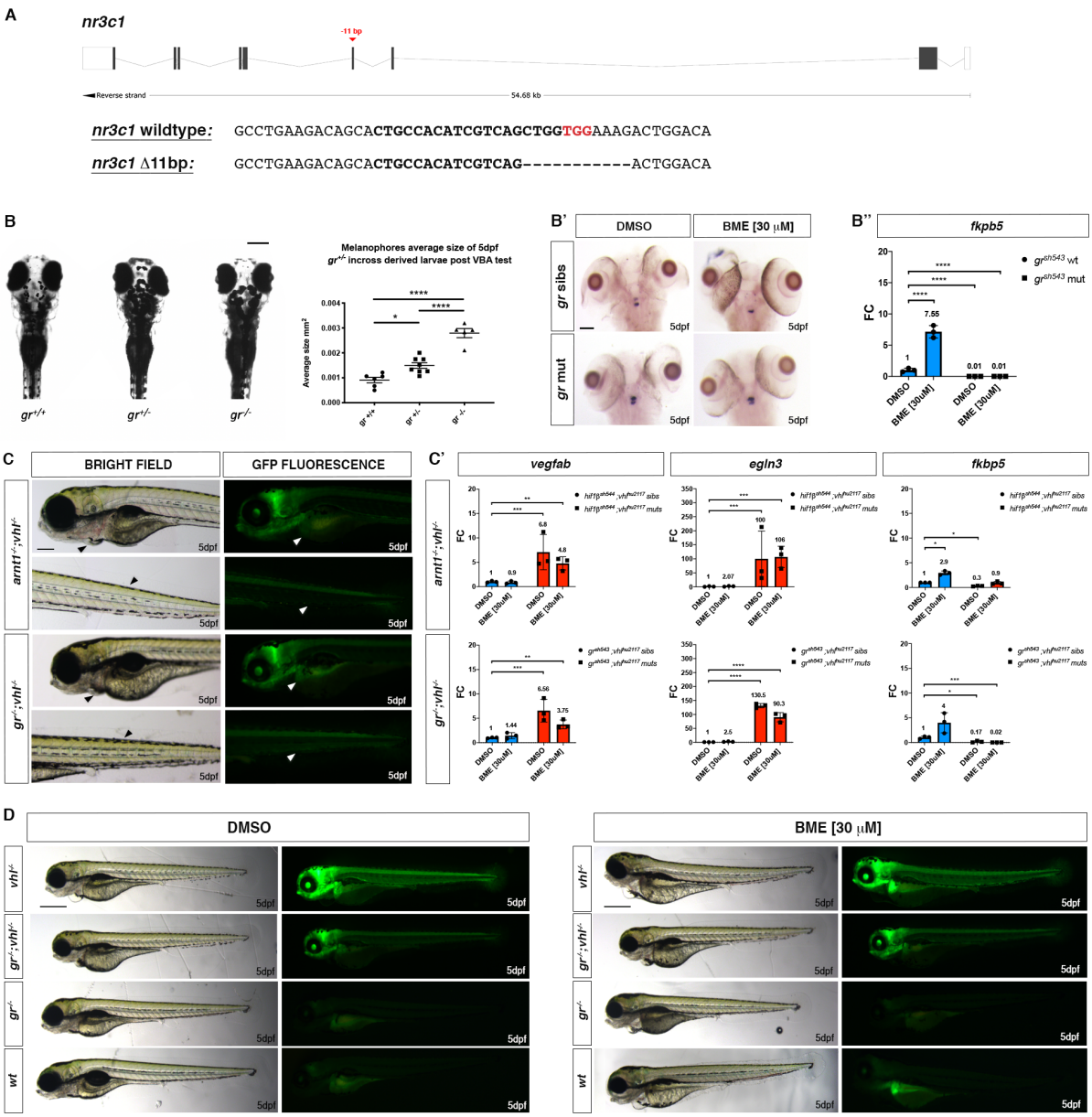

Figure 3. *gr* mutation partially rescues *vhl* phenotype.

A. Schematic representation of zebrafish *gr (nr3c1)* gene. Exons are shown as boxes, introns as lines. The red arrowhead shows the position of a -11 bp deletion in exon 3 (encoding the DNA binding domain). *gr* wt and mutant sequence. CRISPR target site: bold. PAM sequence: red.

B-B''. Tests performed on *gr* mutant line to verify loss of function.

B. VBA test performed on $gr^{+/-}$ incross-derived 5 dpf larvae (n=240), followed by genotyping. Statistical analysis was performed on melanocytes average area (mean ± s.e.m.) of 5 dpf larvae post VBA test. Scale bar 200 μm. Wild-types melanocyte size 0.0009 ± 0.001 mm^2 (P= 0.0123, n=6 larvae), heterozygous: 0.0015 ± 0.0001 mm^2 (P<0.0001, n=8 larvae) and mutant: 0.0028 ± 0.0002 mm^2 (P<0.0001, n=5 larvae). Ordinary One-way ANOVA followed by Sidak's multiple comparisons test.

B'. Representative pictures of WISH performed on DMSO and BME [30 μM] treated *gr* mutant line, at 5 dpf, using *pomca* as probe. Scale bar 100 μm. *gr* siblings DMSO treated (n= 30/30 larvae) showed normal expression; gr siblings (n= 29/30 larvae) showed downregulated pomca expression after BME treatment. Both DMSO treated (n= 30/30) and BME treated (n= 30/30) $gr^{-/-}$ larvae showed upregulated *pomca* expression.

B''. RTqPCR analysis performed on *gr* wt (n=10; 3 repeats) and $gr^{-/-}$ (n=10; 3 repeats) larvae at 5 dpf, using *fkbp5* as probe. Statistical analysis was performed on ΔΔCt values, whereas data are shown as fold change values. Ordinary Two-way ANOVA followed by Dunnett's multiple comparison test (****P < 0.0001).

C. Magnified picture of representative $gr^{-/-}$; $vhl^{-/-}$ larvae compared to $arnt1^{-/-}$;$vhl^{-/-}$ larvae, Both double mutants are characterized by the absence of pericardial oedema, no ectopic extra vasculature at the level of the tail, no bright liver and a reduced brightness in the rest of the body (white and black arrowheads). Fluorescence, exposure = 2 seconds. Scale bar 200 μm.

C'. RTqPCR analysis performed on both HIF and GC target gene expression carried out on both $gr^{-/-}$; $vhl^{-/-}$ and sibling, at 5 dpf, (n=10 larvae, per group, in triplicate) compared to $arnt1^{-/-}$;$vhl^{-/-}$ larvae and siblings, at 5dpd (n=10 larvae, per group, in triplicate). Statistical analysis was performed on ΔΔCt values, whereas data are shown as fold change values, Ordinary Two-way ANOVA followed by Dunnett's multiple comparison test.

D. Representative picture of phenotypic analysis performed on DMSO and BME [30 μM] treated $gr^{+/-}$; $vhl^{+/-}$*(phd3::EGFP)* incross-derived 5 dpf larvae (n=600). Among the 450 GFP^+ larvae analysed, 28 showed a partially rescued *vhl* phenotype which resembled the arnt1's one. Three experimental repeats. In all panels: *P < 0.05; **P < 0.01; ***P <0.001; ****P < 0.0001. Fluorescence, exposure = 2 seconds. Scale bar 500 μm.

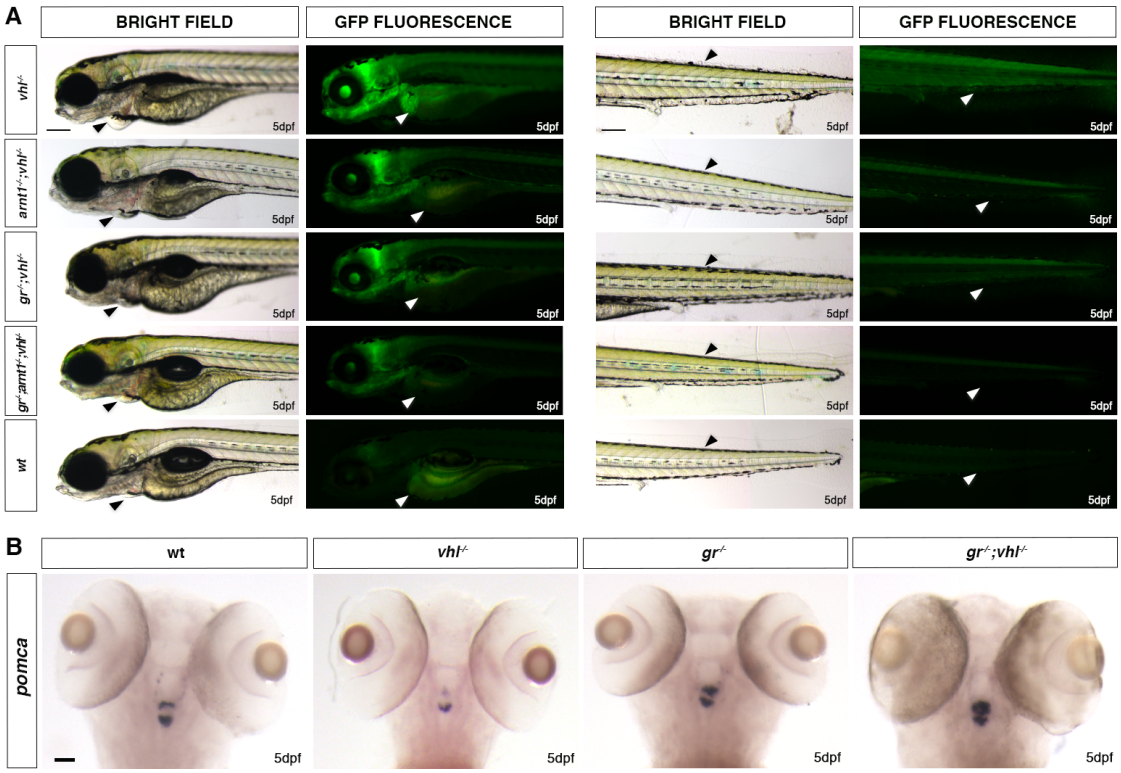

Figure 4. *gr* loss of function effect is stronger when HIF-response is attenuated.

A. Representative picture of the main differences between *vhl*$^{-/-}$, *arnt1*$^{-/-}$;*vhl*$^{-/-}$, *gr*$^{-/-}$;*vhl*$^{-/-}$ *and* triple *gr*$^{-/-}$;*arnt1*$^{-/-}$;*vhl*$^{-/-}$ larvae at 5 dpf. Among the 488 *phd3:eGFP* expressing larvae analysed, 7 larvae were characterized by the absence of pericardial oedema (black arrowheads, left), no ectopic extra vasculature at the level of the tail (black arrowheads, right), no visible *phd3::EGFP* HIF reporter in the liver (white arrowheads, left) and even more reduced levels of this marker in the head and in the rest of the body (white arrowheads, right). Genotypic analysis allowed to confirm the presence of a genotype-phenotype correlation in 5 out 7 samples and to prove that they were triple mutants. Fluorescence, exposure = 2 seconds. Scale bar 200 µm.

B. Representative pictures of WISH performed on *gr*$^{+/-}$; *vhl*$^{+/-}$ incross derived larvae, at 5 dpf, using *pomca* as probe. Of note, *gr*$^{-/-}$;*vhl*$^{-/-}$ showed upregulated *pomca* expression (20/20 larvae), as observed in *gr*$^{-/-}$ (20/20 larvae); *vhl* mutants showed downregulated *pomca* expression (20/20 larvae), whereas wildtypes showed normal pomca expression (19/20). Chi-square test (****P < 0.0001). Scale bar 50 µm.

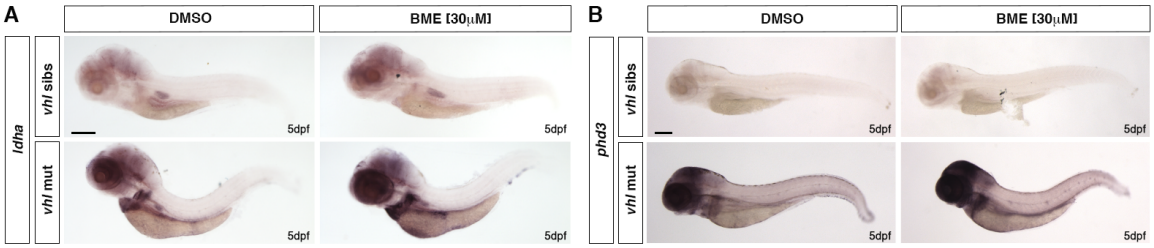

Figure 5. BME treatment is able to induce HIF response in *vhl*$^{-/-}$.

A. Representative pictures of WISH performed on DMSO and BME [30 μM] treated *vhl*$^{+/-}$ incross derived larvae, at 5 dpf, using *ldha* as probe. DMSO treated *vhl* siblings showed basal *ldha* expression (34/35 larvae), which showed to be upregulated after BME treatment (33/35 larvae). On the other hand, DMSO treated *vhl*$^{-/-}$ showed upregulated *ldha* expression (32/35 larvae), which was further upregulated after BME treatment (34/35 larvae). Chi-square test (****P < 0.0001). Scale bar 200 μm.

B. Representative pictures of WISH performed on DMSO and BME [30 μM] treated *vhl*$^{+/-}$ incross derived larvae, at 5 dpf, using *phd3 (egln3)* as probe. As expected, *vhl* siblings DMSO treated (n= 30/30 larvae) showed basal *phd3* expression, which was mildly increased after BME treatment (n= 27/30 larvae). *Vhl*$^{-/-}$ DMSO treated (n= 28/30 larvae) showed upregulated *phd3* expression, which was further increased after BME treatment (n= 26/30 larvae). Chi-square test (****P < 0.0001). Scale bar 200 μm.

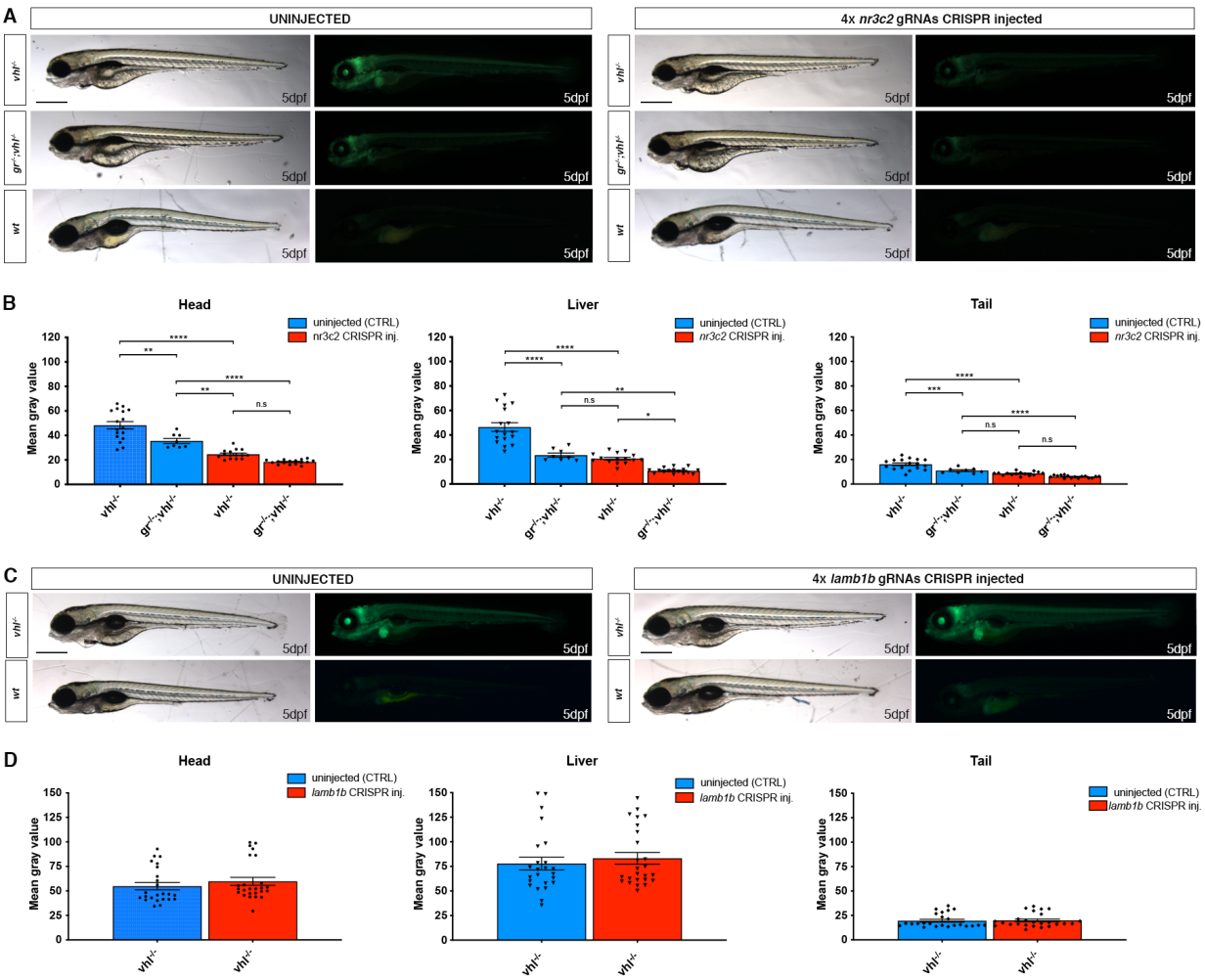

Figure 6. Both Gr and Mr are directly required for assuring proper HIF response.

A. Representative pictures of 5 dpf CRISPANT mutants created by redundantly targeting *nr3c2* (*mr*) gene via co-injection of 4x gRNAs in *gr*$^{+/-}$;*vhl*$^{+/-}$(*phd3:eGFP*) x *gr*$^{-/-}$; *vhl*$^{+/-}$(*phd3:eGFP*) derived embryos (n=344). Uninjected embryos were used as control (n=170). Fluorescence, exposure = 991,4 ms. Scale bar 500 μm.

B. Statistical analysis performed on mean grey value quantification (at the level of the head, liver and tail), after phenotypic analysis, on 5 dpf *mr* 4x gRNAs injected and uninjected larvae. *vhl*$^{-/-}$ uninjected n = 17 larvae: head 48.28 ± 2.99 (mean ± s.e.m); liver 46.47 ± 3.55 (mean ± s.e.m); tail 16.15 ± 1.06 (mean ± s.e.m). *gr*$^{-/-}$;*vhl*$^{-/-}$ uninjected n = 8 larvae: head 35.48 ± 2.03 (mean ± s.e.m); liver 23.56 ± 1.72 (mean ± s.e.m); tail 10.98 ± 0.75 (mean ± s.e.m). *vhl*$^{-/-}$ injected n = 15 larvae: head 24.62 ± 0.97 (mean ± s.e.m); liver 20.67 ± 1.1 (mean ± s.e.m); tail 8.57 ± 0.39 (mean ± s.e.m). *gr*$^{-/-}$;*vhl*$^{-/-}$ injected n = 16 larvae: head 18.33 ± 0.46 (mean ± s.e.m); liver 10.71 ± 0.56 (mean ± s.e.m); tail 6.07 ± 0.26 (mean ± s.e.m); ordinary One-way ANOVA followed by Sidak's multiple comparison test.

C. Representative pictures of 5 dpf CRISPANT mutants created by redundantly targeting *lamb1b* gene via co-injection of 4x gRNAs in *vhl*$^{+/-}$(*phd3:eGFP*) incross-derived embryos (n=400). Uninjected embryos were used as control (n=470). Fluorescence, exposure = 991,4 ms. Scale bar 500 μm.

D. Statistical analysis performed on mean grey values quantification (at the level of the head, liver and tail), after phenotypic analysis on 5 dpf *lamb1b* 4x gRNAs injected and uninjected *vhl*$^{+/-}$(*phd3:eGFP*) incross-derived larvae. *vhl*$^{-/-}$ uninjected n = 24 larvae: head 54.83 ± 3.68 (mean ± s.e.m); liver 77.86 ± 6.46 (mean ± s.e.m); tail 19.56 ± 1.43 (mean ± s.e.m). *vhl*$^{-/-}$ injected n = 25 larvae: head 59.74 ± 4.05 (mean ± s.e.m); liver 83.23 ± 5.92 (mean ± s.e.m); tail 19.9 ± 1.38 (mean ± s.e.m); unpaired t-test (all panels: *P < 0.05; **P < 0.01; ***P <0.001; ****P < 0.0001).